

Minimizing Total Travel Time for Collaborative Package Delivery with Heterogeneous Drones

Thomas Erlebach* Kelin Luo† Wen Zhang†

Abstract

Given a fleet of drones with different speeds and a set of package delivery requests, the collaborative delivery problem asks for a schedule for the drones to collaboratively carry out all package deliveries, with the objective of minimizing the total travel time of all drones. We show that the best non-preemptive schedule (where a package that is picked up at its source is immediately delivered to its destination by one drone) is within a factor of three of the best preemptive schedule (where several drones can participate in the delivery of a single package). Then, we present a constant-factor approximation algorithm for the problem of computing the best non-preemptive schedule. The algorithm reduces the problem to a tree combination problem and uses a primal-dual approach to solve the latter. We have implemented a version of the algorithm optimized for practical efficiency and report the results of experiments on large-scale instances with synthetic and real-world data, demonstrating that our algorithm is scalable and delivers schedules of excellent quality.

1 Introduction

The rise of autonomous vehicle technology has profoundly transformed the logistics and delivery industry, enabling faster and more efficient package delivery. Given the varying serving speeds, consumption costs, and service areas of different vehicles or drones, one of the key challenges in this domain is optimizing the delivery process, particularly when multiple vehicles are available to complete pickup and delivery tasks [14]. This class of problems, known as Collaborative Delivery Problems (CD Problems), focuses on finding an optimal schedule to transport packages from one location to another through the collective effort of multiple vehicles. There are two modes in which vehicles can collaborate on completing the pickup and delivery tasks: In *coarse-grained* collaboration, the vehicles collaborate by partitioning the package delivery requests among themselves: Each package delivery request is assigned to one vehicle, and each of the vehicles independently follows a route based on its assigned requests. In

*Department of Computer Science, Durham University, UK

†Department of Computer Science and Engineering, University at Buffalo, USA

fine-grained collaboration, multiple vehicles can participate in the fulfillment of a single request: The vehicles can collaborate by handing off packages between agents to enhance efficiency and reduce delivery time.

In this paper, we study the multi-package delivery problem in a collaborative setting. We extend the classical problem of multiple vehicle pickup to a setting where the available vehicles have different efficiencies, particularly in terms of speed. We formulate this problem as a Heterogeneous Collaborative Delivery Problem and investigate how delivery planning can be optimized to minimize the objective of total travel time. We use the terms ‘drone’ and ‘vehicle’ interchangeably in the remainder of the paper.

Our contributions can be summarized as follows: (1) We analyze the effectiveness of fine-grained collaboration among vehicles. Our results demonstrate that the benefit of fine-grained collaboration is limited. Specifically, we show that the gap between serving packages with fine-grained collaboration (possibly involving multiple vehicles in the delivery of a single package) and serving them with coarse-grained collaboration (serving each package with a single vehicle) is bounded by a constant factor. (2) The main contribution of this paper is a constant-factor approximation algorithm for the Heterogeneous CD problem with coarse-grained collaboration. We reduce the problem to a Tree Combination Problem and adapt a primal-dual algorithm presented for the multiple-vehicle TSP to address the latter problem. Our model accounts for the heterogeneous capabilities of vehicles and achieves a constant approximation ratio for minimizing total travel time (or total cost). Furthermore, our reduction shifts the problem complexity to depend primarily on the number of vehicles rather than the number of requests, which is typically much larger than the number of vehicles. This advancement offers a practical framework for optimizing real-world routing problems, where variations in vehicle capabilities play a critical role. (3) We describe an optimized implementation of our algorithm and report experimental results regarding running time and solution quality for a range of synthetic and real-world instances. Compared to a baseline heuristic without approximation guarantee, our algorithm produces solutions of comparable and sometimes substantially better quality while displaying a significantly reduced running time.

The remainder of the paper is structured as follows. Section 1.1 discusses related work. Section 2 introduces relevant notation and definitions. Section 3 proves that the gap between fine-grained and coarse-grained schedules is bounded. In Section 4, we present our constant-factor approximation algorithm for the heterogeneous CD problem with coarse-grained collaboration. In Section 5, we describe the optimizations we have applied for the implementation of the algorithm. Then, Section 6 presents the experimental results. Conclusions are given in Section 7.

1.1 Related Work

Collaboration on a Single Request. The problem of delivering a single package has been well studied [2, 3, 4]. These studies consider a problem where

k agents, initially located at distinct nodes of an undirected graph with n nodes and weighted edges, must collaboratively deliver a single item from a source node s to a target node t . The agents can traverse the graph edges starting at time 0, with each agent i moving at a specific velocity ν_i and energy consumption rate w_i . The objective of minimizing total consumption cost was first studied by Bärtschi et al. [2], who provided an $O(n^3)$ algorithm to find the optimal solution. The objective of minimizing delivery time was first addressed by Bärtschi et al. [3], who proposed an algorithm with time complexity $O(k^2m + kn^2 + \text{APSP})$, where APSP refers to the time required to compute all-pairs shortest paths in a graph with n nodes and m edges. Later, Carvalho et al. [4] improved the time complexity for this problem to $O(kn \log n + km)$. All these results are based on the common assumption that every agent can travel freely throughout the entire graph without any restrictions.

Studies on collaboration for a single request also explore scenarios where each agent’s travel distance is limited [5, 6], where an agent’s overall movement is restricted [9], or even where the package’s path is restricted [7]. The problem in which each agent has an energy budget that constrains its total distance traveled has been shown to be strongly NP-hard in general graphs [5]. Scenarios where each agent is constrained to a specified movement subgraph have been studied for both minimizing total consumption and total delivery time, and it has been shown to be NP-hard [9]. The variant in which the package must travel via a fixed path in a general graph has been studied by Chalopin et al. [7].

Collaboration on Two or More Requests. Although significant progress has been made, particularly with the proposal of fast polynomial-time algorithms, in understanding collaborative delivery in single-package scenarios, the problem becomes computationally challenging once multiple packages are introduced [2]. In fact, even with just two packages, the minimum delivery time collaborative delivery problem, without any additional restrictions, is already NP-hard [4].

Dial a Ride. The Dial-a-Ride Problem (DARP)—in both its preemptive and non-preemptive forms—involves a set of objects (each specified by a source-destination node pair) and a fleet of vehicles. The objective is to compute the shortest possible tour such that all objects are picked up from their sources and delivered to their destinations, without exceeding the vehicle’s capacity at any point in time. This problem is typically studied under capacity constraints, with the common assumption that all vehicles are homogeneous. Our problem can be viewed as a heterogeneous, unit-capacity, non-preemptive DARP. While Frederickson et al. [10] gave a 1.8-approximation for the unit-capacity case on general graphs, the heterogeneous setting, to the best of our knowledge, remains unexplored.

Heterogeneous TSP. A special case of our problem, where the pickup location equals the drop-off location, can be viewed as a Multiple Depot Hetero-

geneous Traveling Salesman Problem (MDHTSP), since each package delivery is considered completed as soon as its corresponding node is visited, with only the minor difference that vehicles need to return to their depots in the MDHTSP. Rathinam et al. [13] present a 2-approximation algorithm for MDHTSP based on the primal-dual method. Our algorithm also leverages the primal-dual method, with an extension of their method.

2 Preliminaries

We are given a metric space (X, d) , where $d : X \times X \rightarrow \mathcal{R}_{\geq 0}$ is a distance function satisfying the triangle inequality. A set of vehicles (or drones) K with $k = |K|$ is specified, where each drone $j \in K$ has a depot (or initial location) $r_j \in X$ and a speed p_j . To traverse from node $u \in X$ to node $w \in X$, drone j takes time $\frac{d(u,w)}{p_j}$. Without loss of generality, we assume that for any two drones i and j with $i < j$, the speed satisfies $p_i \geq p_j$. We are also given a set of m packages to be delivered, each specified by a pickup location $s_i \in X$ and a drop-off location $t_i \in X$. We use the terms *package* and *s-t* pair interchangeably. Each drone can carry at most one package at a time.

One of the main objective functions in collaborative delivery problems is the total completion time, also known as the sum of completion times. For a given solution, the completion time is computed for every drone, and the objective function value is the sum of all these values. The task of our problem is to find a schedule for delivering all the packages from the start node to the destination node while minimizing the total completion time.

We define a schedule π_j for drone j as an ordered (by pickup time t) set of triples $\{(u_i, w_i, t)\}$, where the drone picks up package P_i at location u_i at time t and delivers it to location w_i . For any two consecutive triples in the schedule $\{(u_i, w_i, t)\}$ and $\{(u_{i'}, w_{i'}, t')\}$, the pickup time of the second must be at least the previous pickup time plus the travel time from u_i to w_i and from w_i to $u_{i'}$. The time t of the first triple $\{(u_i, w_i, t)\}$ in π_j must be at least the time it takes the drone to travel from its depot r_j to u_i .

The schedule for each package P_i can be obtained by collecting all triples involving package i , i.e., $\bar{\pi}_i = \{(u_i, w_i, t), \dots\}$, from the union of all drone schedules $\bigcup_j \pi_j$, and sorting them by the associated time t . Note that for each package P_i , the first triple should have $u_i = s_i$, and the final triple should have $w_i = t_i$; these may be the same triple. A package can only be picked up at a location u_i if it is the source s_i , or after it has been dropped off at u_i by another drone (or the same drone) at an earlier time.

Definition 2.1 (Min-Sum Collaborative Delivery Problem (Min-Sum CD Problem)). *Given a metric space (X, d) , a set of m packages $\mathcal{P} = \{s_i, t_i\}_{i=1}^m$ where s_i is the pick-up location and t_i is the drop-off location, and k drones each with a depot r_j and speed p_j for each drone j , the goal is to find schedules (or routes) $\{\pi_j\}_{j \in [k]}$ such that the schedule for each drone j originates at its initial location r_j , and each package i is transported from its source s_i to its destination t_i . The*

objective is to minimize the total cost, defined as the sum of travel times across all drone routes:

$$\sum_{j=1}^k \left(t_{f_j} + \frac{d(u_{f_j}, w_{f_j})}{p_j} \right),$$

where $(u_{f_j}, w_{f_j}, t_{f_j})$ is the final triple in the schedule π_j of drone j . Note that drone j finishes its schedule at time $t_{f_j} + \frac{d(u_{f_j}, w_{f_j})}{p_j}$ because t_{f_j} is the time at which it makes its final pick-up (at location u_{f_j}), and then its final move is to take the package P_{f_j} from u_{f_j} to w_{f_j} with speed p_j .

We consider Min-Sum CD with both fine-grained and course-grained collaboration. In the remainder of the paper, we refer to these variants of the problem as the preemptive and the non-preemptive variant, respectively.

Definition 2.2 (Preemptive vs Non-preemptive). *Considering the output routes, we have the following two versions of Min-Sum CD:*

- In the preemptive Min-Sum CD problem, after picking up a package from its source, it may (repeatedly) be left at an intermediate location before being picked up by another (or the same) drone and transported further on its route to the destination. In this case, the schedule for each package may include multiple triples.
- In the non-preemptive Min-Sum CD problem, a package, once picked up from its source, is carried by the drone until it is dropped off at its destination. In this case, the schedule for each package includes only a single triple (s_i, t_i, t) .

In this paper, our focus will be on designing algorithms for the *non-preemptive Min-Sum CD* problem, as we can demonstrate that the impact of preemption on the Min-Sum CD problem is limited: We show in the following section that the gap between the cost of the optimal preemptive and non-preemptive tours is no more than a constant factor.

3 From Preemptive to Non-preemptive

We show that the gap between the optimal collaborative preemptive and non-preemptive tours is bounded.

Theorem 3.1. *An optimal schedule for the preemptive Min-Sum CD problem with total cost OPT can be transformed into a non-preemptive schedule with cost at most $3 \cdot \text{OPT}$.*

Proof. Consider an optimal schedule Π^* for the *Preemptive Min-Sum CD* problem, with π_i^* denoting the schedule of drone i in the optimal schedule. The cost of this optimal preemptive solution, OPT, also serves as a lower bound for the optimal solution to the *Non-preemptive Min-Sum CD* problem. Given

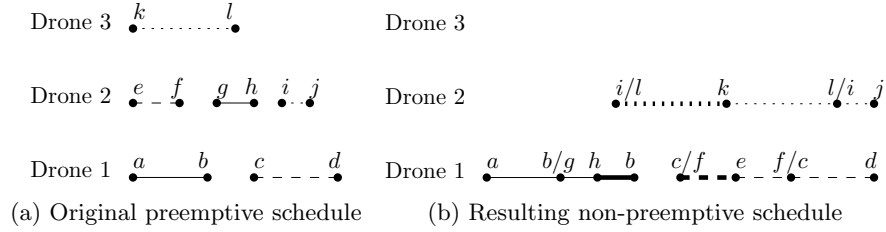


Figure 1: Consider the preemptive schedule with three drones in Figure (a), represented by solid, dotted, and dashed lines, corresponding to three different packages, respectively. Drones 2 and 3 are involved in parts of the dotted package schedule, while drones 1 and 2 are involved in parts of both the dashed and the solid package schedules. Note that points b/g , c/f , and i/l are co-located. In the constructed non-preemptive schedule in Figure (b), additional travel distances are incurred for each package due to a drone deviating from its original route—either to pick up a package or to return to a point where it can resume its original schedule after a delivery. These additional distances are represented by thicker lines matching the style of the corresponding package in Figure (b). For the solid package, the fastest drone, drone 1, first serves the sub-path $a \rightarrow b$, then the sub-path $g \rightarrow h$ to complete the delivery, and finally returns to point b to resume the original schedule. For the dashed package, drone 1 travels from point c (which shares the location with f) to the pickup point e , then serves the sub-path $e \rightarrow f$ followed by the sub-path $c \rightarrow d$ to complete the delivery.

an optimal schedule $\Pi^* = \{\pi_i^*\}_{i \in [k]}$, we construct a feasible schedule for the non-preemptive Min-Sum CD problem with value at most $3 \cdot \text{OPT}$.

The construction of a feasible non-preemptive schedule Π from Π^* is done via the following algorithm. Recall that the drones are indexed by non-increasing speed.

Algorithm 1 Reducing a preemptive solution to a non-preemptive solution

- 1: $\Pi = \emptyset$, $i = 1$.
 - 2: **while** $i \leq k$ **do**
 - 3: Obtain from π_i^* a schedule π_i serving all unscheduled packages in the order of serving in π_i^* .
 - 4: Set $\Pi \leftarrow \Pi \cup \{\pi_i\}$ and $i \leftarrow i + 1$.
 - 5: **end while**
-

The schedules π_i^* that constitute OPT are processed in increasing order of i , i.e., the schedule of the fastest drone is processed first and that of the slowest drone last. We say a drone serves package j if it carries j at least once during its path. Assume drone i serves k_i different packages $P_{i_1}, \dots, P_{i_{k_i}}$, indexed in the order in which i picks them up the first time, that aren't served by any drone i'

with $i' < i$. For each $1 \leq j \leq k_i$, assume drone i picks up P_{i_j} at vertex v_{i_j} and drops it off at w_{i_j} the first time it carries P_{i_j} . For each j with $1 \leq j \leq k_i$, we modify the tour of drone i as follows: after reaching v_{i_j} , the drone moves to s_{i_j} , picks up P_{i_j} there, carries it directly to t_{i_j} , then moves to w_{i_j} and continues its original tour. After processing π_i^* in this way to obtain a schedule π_i for drone i , the packages $P_{i_1}, \dots, P_{i_{k_i}}$ are served non-preemptively by drone i . If $i < k$, we proceed to handle drone $i + 1$ in the same way. Figure 1 gives an example of preemptive tours and the constructed non-preemptive tours.

The algorithm transforms an optimal preemptive solution $\{\pi_i^*\}_{i \in [k]}$ into a feasible non-preemptive one $\{\pi_i\}_{i \in [k]}$. For each package P_j , let $i(j)$ denote the fastest drone that serves P_j in the preemptive schedule. Let $\bar{\pi}_j^*$ represent the set of triplets involving package P_j that are traversed in the preemptive schedule, and let $w(\bar{\pi}_j^*)$ denote the total length of these triplets. Then $\sum_j (w(\bar{\pi}_j^*)/p_{i(j)})$ is a lower bound on the total cost of the preemptive solution, as package P_j is served only by drone $i(j)$ and slower drones. When transforming the solution into a feasible non-preemptive one using the algorithm described above, the increase in the total cost is at most $\sum_j (2w(\bar{\pi}_j^*)/p_{i(j)}) \leq 2\text{OPT}$. This is because letting drone $i(j)$ that originally serves only the subpath of $\bar{\pi}_j^*$ from some v_j to some w_j in the preemptive solution now serve the whole package P_j requires extra trips from v_j to s_j and back, and from w_j to t_j and back. This results in an increase in total distance of at most $2w(\bar{\pi}_j^*)$, because the total length of the subpaths from v_j to s_j and from w_j to t_j is at most $w(\bar{\pi}_j^*)$ as these subpaths are disjoint parts of $\bar{\pi}_j^*$. In conclusion, the constructed non-preemptive solution has total cost at most $3 \cdot \text{OPT}$ because the original preemptive solution has cost at most OPT and the increase in the total cost when transforming the solution into a non-preemptive one is at most $2 \cdot \text{OPT}$. \square

Theorem 3.1 implies the following.

Corollary 3.2. *An α -approximation algorithm for the Non-preemptive Min-Sum CD problem implies a 3α -approximation algorithm for the Preemptive Min-Sum CD problem.*

The following lemma shows that the total length of all shortest package routes, divided by the speed of the fastest drone, is a lower bound on the optimal cost of the Min-Sum CD problem.

Lemma 3.3. *Let an instance I of Preemptive or Non-preemptive Min-Sum CD be given, and let p_1 be the speed of the fastest drone. Then*

$$\frac{\sum_{i=1}^m d(s_i, t_i)}{p_1}$$

is a lower bound on the optimal sum of completion times for I .

Proof. Let Π^* be an optimal solution to instance I . For each $1 \leq i \leq m$, let $\bar{\pi}_i$ denote the set of triplets involving package P_i in Π^* . In the non-preemptive case, $\bar{\pi}_i$ contains only a single triplet (s_i, t_i, t) . In the preemptive case, $\bar{\pi}_i$ may

be a concatenation of triplets handled by multiple drones. The total cost of Π^* is at least $(\sum_{i=1}^m w(\bar{\pi}_i))/p_1$, where $w(\bar{\pi}_i)$ denotes the total length of the triplets in $\bar{\pi}_i$. Since $w(\bar{\pi}_i) \geq d(s_i, t_i)$ for each i , the lemma follows. \square

4 Non-preemptive Min-Sum CD

We first consider the special case where all drones are initially located in the same depot and show that using only the fastest drone provides a constant-factor approximation (Section 4.1). After that, we tackle the general case in Section 4.2.

4.1 Identical Depot Locations

Assume that all drones are located at the same depot. We start with the following lemma.

Lemma 4.1. *Let an instance I of non-preemptive Min-Sum CD where all drones have the same depot location be given. Denote by T a minimum spanning tree for the depot location and the sources of all packages, and use $w(T)$ to denote the sum of its edge lengths. Then $w(T)/p_1$ is a lower bound on the optimal sum of completion times, where p_1 is the speed of the fastest drone.*

Proof. Let $\pi_1^*, \pi_2^*, \dots, \pi_k^*$ be the schedules (or paths) followed by the k drones in an optimal solution. The union of these paths (after short-cutting all nodes that are not depot or packages sources) is a connected graph that contains the depot and the sources of all packages and uses only direct edges between such nodes (as opposed to, say, a Steiner tree that could use additional Steiner nodes to connect the nodes). As the minimum spanning tree has minimum total length among all such connected graphs, the total length of the edges of those paths is at least $w(T)$. Since no drone has speed larger than p_1 , the total completion time of the optimal solution is at least $w(T)/p_1$. \square

Theorem 4.2 (Min-Sum CD with Identical Depot Locations). *There is a 4-approximation algorithm for the non-preemptive Min-Sum CD problem when all drones have the same depot location.*

Proof. The algorithm first computes a minimum spanning tree T for the depot and all source locations. Then it doubles every edge of T and creates a Eulerian tour π of T . Next, it attaches to each package source s_i at its first occurrence in π the edges (s_i, t_i) (to deliver package P_i) and (t_i, s_i) (to return to s_i), yielding the tour π' . Finally, using the fastest drone to follow tour π' starting at the depot and ending when the last package is delivered is output as the solution.

The sum of completion times of the solution is equal to the completion time of the fastest drone, as no other drone is used. The completion time of the fastest drone is at most

$$\frac{d(\pi')}{p_1} \leq \frac{2w(T) + 2 \sum_{i=1}^m d(s_i, t_i)}{p_1},$$

which is bounded by $2\text{OPT} + 2\text{OPT} = 4\text{OPT}$ by Lemmas 4.1 and 3.3. \square

4.2 Arbitrary Depot Locations

We translate the Min-Sum CD problem into a certain tree combination problem. An instance of the tree combination problem consists of a set of trees, referred to as *original trees*, each associated with a drone speed p_i . We can add edges to connect different trees. A tree formed by a number of original trees together with the edges that have been added to connect them into a single tree is called a *large tree*. For every large tree T , the cost of T is defined to be the total edge length of T divided by the fastest drone speed associated with any of the original trees that are included in T .

Definition 4.3 (Tree Combination Problem). *Given a metric space (V, d) and a set of trees $\mathcal{T} = T_1, T_2, \dots, T_k$, where $V(T_i) \subseteq V$ and each tree T_i is rooted at a drone location $r_i \in V$ with a corresponding drone speed p_i , the objective is to combine trees so as to minimize the sum, over all the resulting large trees, of the total edge length of the large tree divided by the highest speed among the drones associated with the original trees included in the large tree.*

Lemma 4.4 (Reducing Min-Sum CD to a Tree Combination Problem). *Every given instance of the Min-Sum CD problem can be reduced in polynomial time to an instance of the Tree Combination Problem such that an α -approximation algorithm for the Tree Combination Problem implies a 6α -approximation algorithm for the Min-Sum CD problem.*

Proof. Given an instance of the min-sum CD problem, we construct an instance of the tree combination problem with the following algorithm:

Algorithm 2 Constructing Trees $((V, d), \{s_i, t_i\}_{i \in [m]}, \{r_i\}_{i \in [k]})$

- 1: Create a new graph G' from the metric $(\{s_i\}_{i \in [m]} \cup \{r_i\}_{i \in [k]}, d)$ by contracting the set of depots $R = \{r_1, r_2, \dots, r_k\}$ into a single node r .
 - 2: Compute the minimum spanning tree (MST) T of the graph G' .
 - 3: Obtain the forest $\{T_i\}_{i \in [k]}$ from T by un-contracting the node r back into the original depots in R , such that each tree T_i in the forest is rooted at a distinct depot r_i .
 - 4: For each package source vertex s_i , connect vertex t_i to s_i in its respective tree.
-

The algorithm begins by contracting all depots into a single node. Specifically, this involves: (i) introducing a new node r and removing the depots in R , (ii) for each depot $r_i \in R$, every edge (s, r_i) (for every source s) induces an edge (s, r) , and (iii) setting $d(s, r) = \min_{i \in [k]} d(s, r_i)$. The algorithm then computes a minimum spanning tree (MST) in the contracted graph. In Line 3, the MST is broken into a set $\{T_i\}_{i \in [k]}$ of k disjoint trees by un-contracting the nodes in R . This un-contraction means that an edge (s, r) is mapped back to an edge (s, r_i) ,

where $d(s, r) = d(s, r_i)$. Note that, by construction, every tree T_i is rooted at r_i and each vertex is covered in exactly one tree. Tree T_i is associated with drone speed p_i . If several drones are located at the same depot r_i , the drone with the fastest speed among the drones at that depot is chosen.

Note that a solution to the constructed instance of the tree combination problem with objective value x can be used to construct a solution to the non-preemptive Min-Sum CD problem with sum of completion times at most $2x$ as follows: For each large tree T' with highest drone speed p_i , let the drone with speed p_i traverse an Euler tour of T' .

Observation 4.5. *For any subset U of the trees $\{T_i \mid 1 \leq i \leq k\}$, the total length of the optimal tours for the packages contained in trees of U is at least one half of the total length of the trees in U .*

Proof. The total length of the trees in U is equal to the weight of the MST of the subgraph G'' of G' induced by r and all the sources in U , plus the sum of $d(s_j, t_j)$ for all packages P_j whose source s_j is in U . Let Π^* be optimal tours for serving the packages whose sources are in U . For each tour π^* in Π^* , consider the *shortened tour* obtained from π^* by only visiting the sources on π^* and short-cutting all other nodes. The union of these shortened tours forms a spanning subgraph of G'' and hence has total length at least the weight of the MST of G'' . Therefore, the weight of the MST is at most the total length of the shortened optimal tours, and hence at most the total length of the optimal tours. Furthermore, a separate path of length at least $d(s_j, t_j)$ must be included in the tours in Π^* for each package with s_j in U . Hence, the total length of the optimal tours is at least the sum of $d(s_j, t_j)$ over all packages P_j with s_j in U . This shows that the total length of the trees in U is at most twice the total length of the optimal tours. •

Let $\Pi^* = \{\pi_1^*, \pi_2^*, \dots, \pi_k^*\}$ be an optimal schedule, with total cost OPT, for the given instance of the min-sum CD problem. If the package paths of each constructed tree T_i are entirely contained within one of the optimal tours, and if the drone used to execute an optimal tour is one of the drones associated with a tree T_i whose packages that tour serves, then the lemma can be proved as follows. Consider one optimal tour π_j^* , and let U_j denote the set of trees T_i that are served by π_j^* . We combine the trees in U_j into a large tree T'_j , using the edges of an MST in the graph H on U_j where every tree T_i in U_j is contracted to a single node. The total length of the edges used for the combination is at most the length of the tour π_j^* , as π_j^* induces a connected subgraph of H . Hence, by Observation 4.5, the total length of T'_j is at most 3 times the total length of π_j^* . As the same argument holds for every optimal tour π_j^* , the constructed solution to the tree combination problem has objective value at most 3OPT . An α -approximation algorithm for the tree combination problem hence produces a solution with objective value at most $3\alpha\text{OPT}$, giving a solution with total cost at most $6\alpha\text{OPT}$ for the non-preemptive Min-Sum CD problem.

In the general case, we can apply the following combination procedure to obtain a solution to the tree combination problem, for which we can show that the cost is at most three times the cost of the optimal solution to the Min-Sum

CD problem. We say that a tour π_j or a tree T_j is *trivial* if it serves no packages and *non-trivial* otherwise. In other words, a tour π_j or tree T_j is trivial if the drone from that depot is not used to serve any packages.

Algorithm 3 Construct Large Trees ($\{\pi_i^*\}_{i \in [k]}, \{T_i\}_{i \in [k]}$)

```

1: for  $j = 1$  to  $k$  do
2:   if  $\pi_j^*$  is non-trivial or  $T_j$  is non-trivial and has not yet been merged then
3:     set  $\Pi = \{\pi_j^*\}$  and  $\mathcal{T} = \{T_j\}$ 
4:     while the set of packages served in  $\Pi$  and  $\mathcal{T}$  are different do
5:       if there exists a package  $l$  served by a tour in  $\Pi$  that is not served
        by one of the trees in  $\mathcal{T}$  then
6:         let  $T_i$  (necessarily  $i > j$ ) be the tree that serves  $l$ 
7:         insert  $T_i$  into  $\mathcal{T}$ 
8:         insert  $\pi_i^*$  into  $\Pi$ 
9:       end if
10:      if there exists a package  $l$  served by a tree in  $\mathcal{T}$  that is not served
        by one of the tours in  $\Pi$  then
11:        let  $\pi_i^*$  (necessarily  $i > j$ ) be the tour that serves  $l$ 
12:        insert  $\pi_i^*$  into  $\Pi$ 
13:        insert  $T_i$  into  $\mathcal{T}$ 
14:      end if
15:    end while
16:    form a large tree  $L_i$  from the trees in  $\mathcal{T}$  (using an MST computation
        to find edges of minimum total length to be added) and add it to the solution
17:  end if
18: end for

```

Assume Algorithm 3 constructs ℓ large trees. Denote these large trees by $L_{i_1}, L_{i_2}, \dots, L_{i_\ell}$ with $1 \leq i_1 < i_2 < \dots < i_\ell \leq k$, where any large tree L_{i_q} consists of tree T_{i_q} and some number of trees T_j for $j > i_q$. Let $\mathcal{T}(L_{i_q})$ denote the set of these trees. Note that L_{i_q} serves the packages served by $\pi_{i_q}^*$ and some number of tours π_j^* for $j > i_q$. Let $\Pi(L_{i_q})$ denote the set of optimal tours whose packages L_{i_q} serves. Note that the sets $\mathcal{T}(L_{i_q})$ of trees form a partition of the original set of trees, that the sets $\Pi(L_{i_q})$ form a partition of the set of optimal tours, and that the set of indices of the trees in $\mathcal{T}(L_{i_q})$ is the same as the set of indices of the optimal tours in $\Pi(L_{i_q})$. At the point Algorithm 3 forms the large tree L_{i_q} , the variables \mathcal{T} and Π correspond to $\mathcal{T}(L_{i_q})$ and $\Pi(L_{i_q})$, respectively.

By Observation 4.5, the total length of the trees T_j in $\mathcal{T}(L_{i_q})$ is at most twice the total length of the tours in $\Pi(L_{i_q})$. Furthermore, the total length of the edges used to merge the T_j in $\mathcal{T}(L_{i_q})$ into the single large tree L_{i_q} is at most the total length of the tours in $\Pi(L_{i_q})$. To see this, we will show the following claim: Whenever a tree T_i and a tour π_i^* get added to \mathcal{T} and Π , respectively, there is a tour π_g^* in Π that contains a path from a node in $T_g \in \mathcal{T}$ to a node in T_i . From this claim it then follows that the optimal tours in $\Pi(L_{i_q})$ contain paths that make the trees in $\mathcal{T}(L_{i_q})$ a connected structure and hence have total

length at least the total length of the edges the algorithm chooses to connect those trees into L_{i_q} in Line 16.

To show the claim, first note that throughout the execution of Lines 3–15 it holds that every tree T_i in \mathcal{T} contains the same depot r_i as the corresponding optimal tour π_i^* . Now, if T_i and π_i^* get added in Lines 7–8 because another tour π_g^* in Π serves a package l that is not yet served by a tree in \mathcal{T} , then π_g^* contains a path from r_g to s_l , so π_g^* contains a path connecting T_g and T_i . If T_i and π_i^* get added in Lines 12–13 because a tree T_h in \mathcal{T} serves a package l that is not yet served by an optimal tour in Π and that is served by π_i^* , then π_i^* contains a path from r_i to s_l , which is a path connecting T_i and T_h . Thus, the claim follows.

In the remainder of the proof, we use $\text{len}(E)$ to denote the total length of E , where E can be a tree, a set of trees, a tour, or a set of tours. Furthermore, we define $\text{cost}(E) = \frac{\text{len}(E)}{p_g}$, where p_g is the speed of the drone that serves the requests associated with E and whose identity will be clear from the context. From the discussion above, we obtain that the total length $\text{len}(L_{i_q})$ of the large tree L_{i_q} is at most 3 times the total length $\text{len}(\Pi(L_{i_q}))$ of the tours in $\Pi(L_{i_q})$: The trees in $\mathcal{T}(L_{i_q})$ have total length at most $2 \cdot \text{len}(\Pi(L_{i_q}))$, and the edges used to connect them into a large tree have total length at most $\text{len}(\Pi(L_{i_q}))$.

Next, observe that the large tree L_{i_q} is served by drone i_q , and that this is the fastest of the drones associated with any tree in $\mathcal{T}(L_{i_q})$, and thus also the fastest of the drones associated with any of the optimal tours in $\Pi(L_{i_q})$. We thus have

$$\begin{aligned} \text{cost}(L_{i_q}) &= \frac{\text{len}(L_{i_q})}{p_{i_q}} \leq \frac{3 \cdot \text{len}(\Pi(L_{i_q}))}{p_{i_q}} = \sum_{\pi_g^* \in \Pi(L_{i_q})} \frac{3 \cdot \text{len}(\pi_g^*)}{p_{i_q}} \\ &\leq \sum_{\pi_g^* \in \Pi(L_{i_q})} \frac{3 \cdot \text{len}(\pi_g^*)}{p_g} = 3 \sum_{\pi_g^* \in \Pi(L_{i_q})} \text{cost}(\pi_g^*) \end{aligned}$$

where the last inequality follows from $p_g \leq p_{i_q}$ for all $\pi_g^* \in \Pi(L_{i_q})$ because $g \geq i_q$. As the sets $\Pi(L_{i_q})$ form a partition of $\{\pi_1^*, \pi_2^*, \dots, \pi_k^*\}$, this implies:

$$\sum_{j=1}^{\ell} \text{cost}(L_{i_j}) \leq 3 \sum_{j=1}^{\ell} \sum_{\pi_g^* \in \Pi(L_{i_q})} \text{cost}(\pi_g^*) = 3 \sum_{g=1}^k \text{cost}(\pi_g^*)$$

Therefore, the total cost of the large trees is at most 3 times the total cost of the optimal tours. Hence, an α -approximation algorithm for the tree combination problem yields a tree combination solution with total cost at most $3\alpha \cdot \text{OPT}$, which then gives a solution to the Min-Sum CD problem with cost at most $6\alpha \cdot \text{OPT}$ as described earlier. \square

Our problem can be reduced to solving the Tree Combination problem, where the input trees are the outputs of Algorithm 2. Without loss of generality, the input consists of k trees, denoted as T_1, T_2, \dots, T_k , where $w(T_i)$ represents the

total length of the tree T_i . Each tree T_i is rooted at a drone location r_i with an associated drone speed p_i .

We introduce some notation for this problem as follows: Let $T = (V, E)$ represent one of the combined trees, where V is a subset of the input trees \mathcal{T} , and E consists of the shortest edges between the corresponding original trees. For an edge $e = (u, v) \in E$ connecting two trees u, v , the edge length $\ell(e)$ in the combined tree T is defined as

$$\ell(e) = \min_{a \in V(u), b \in V(v)} d(a, b)$$

where $V(u)$ and $V(v)$ denote the sets of vertices in the original input trees corresponding to u and v in the combined tree T , respectively. If a tree T contains more than two vertices (original trees), we assume it is rooted at a vertex with the highest speed. For every vertex $v \in V$, we use $V_v \subseteq V$ to denote the set of descendants of v , and v itself. We use $E_v \subseteq E$ to denote all edges that include at least one vertex from the set V_v .

Observation 4.6. *Consider an optimal solution to the Tree Combination Problem with two speeds, $p_1 > p_2$. The following conditions are satisfied:*

1. *Each combined tree (with more than one original tree) contains exactly one tree with high speed (i.e., with speed p_1).*
2. *For a combined tree $T = (V, E)$ and a vertex $v \in V$ different from the root, the total length of edges in E_v is no more than $p_1/p_2 - 1$ times the total length of all vertices in V_v , i.e., $\sum_{e \in E_v} \ell(e) \leq \sum_{u \in V_v} w(u) \cdot (p_1/p_2 - 1)$, where $w(v)$ is the total length of the corresponding original tree for vertex v .*

Proof. The first part of the observation is straightforward: If a combined tree does not contain a tree with the high speed, there is no need to connect these trees, as the total cost would only increase. On the other hand, if there are at least two trees rooted at drones with high speed within a combined tree, we can partition the combined tree into two separate trees by removing an edge connecting two subtrees that both contain a high speed tree. The resulting separated trees will have a lower total cost than the original combined tree since both separated trees contain a high speed tree and the total length is smaller. This contradicts the assumption that the combined tree is optimal in the solution.

To demonstrate the second part of the observation, assume there is a vertex v in the combined tree such that the total length of edges in E_v exceeds $p_1/p_2 - 1$ times the total cost of all vertices in V_v , i.e.,

$$\begin{aligned} \sum_{u \in V_v} w(u) \cdot (p_1/p_2 - 1) &< \sum_{e \in E_v} \ell(e) \\ \sum_{u \in V_v} w(u)/p_2 &< \sum_{u \in V_v} w(u)/p_1 + \sum_{e \in E_v} \ell(e)/p_1 \end{aligned}$$

In this case, we can partition the combined tree into $1 + |V_v|$ trees (one tree T' with high speed and $|V_v|$ trees with slow speed) by removing all edges in E_v . The resulting trees will have a lower total cost than the original combined tree,

$$\frac{w(T')}{p_1} + \sum_{u \in V_v} w(u)/p_2 + w(v)/p_1 < \frac{w(T')}{p_1} + \sum_{u \in V_v} w(u)/p_1 + \sum_{e \in E_v} \ell(e)/p_1,$$

which contradicts the assumption that the combined tree is optimal in the solution. \square

To solve the Tree Combination Problem with two speeds, we consider a Prize Collecting Steiner Tree Problem: Given an undirected graph $G = (V, E)$, edge cost $c_e \geq 0$ for all edges $e \in E$, a set of selected root vertices $R \subset V$, and penalty $\pi_i \geq 0$ for all $i \in V$. The goal is to find a forest F such that each tree in F contains a root vertex $r \in R$, with the objective of minimizing the cost of the edges in F plus the penalties of the vertices not in F , i.e., $\sum_{e \in F} c_e + \sum_{r \in V - V(F)} \pi_i$, where $V(F)$ is the set of vertices in the forest F . The Prize Collecting Steiner Tree problem is normally defined for a single root, but our formulation with a set R of roots is equivalent as the vertices in R can be merged into a single root before an algorithm for the Prize Collecting Steiner Tree problem is applied.

Lemma 4.7 (Reducing the Tree Combination Problem with Two Speeds to a Prize Collecting Steiner Tree Problem). *An α -approximation algorithm for the Prize Collecting Steiner Tree Problem implies an α -approximation algorithm for the Tree Combination problem with two speeds.*

Proof. To formulate the Tree Combination Problem with Two Speeds as a Prize Collecting Steiner Tree Problem, all trees are represented as vertices in the graph $G = (V, E)$, where each vertex corresponds to a tree. The edge between any two trees represents the cost of connecting the nodes corresponding to those trees. Specifically, the cost of an edge is given by the minimum distance between the nodes in the two trees, divided by the higher speed. We designate all trees with high speed as the root vertices $R \subseteq V$, and all trees with slow speed are assigned penalties $\pi_i \geq 0$ for all $i \in V$. Specifically, the penalty for each vertex is given by the difference in the inverses of the speeds multiplied by the total length of the tree, which represents the cost incurred if the vertex is not connected to a high-speed tree. The goal is to find a forest F that contains multiple trees, each rooted at a node corresponding to a tree with high speed. The objective is to minimize the sum of the costs of the edges in F and the penalties of the vertices not included in the forest F .

The original Tree Combination Problem aims to minimize both the connection cost and the serving cost for each tree. In contrast, the constructed instance of the Prize Collecting Steiner Tree Problem focuses on the connection cost and only a partial serving cost for each tree. Specifically, for trees with high speed and slow-speed trees connected to a high-speed tree, the serving cost is not considered. For slow-speed trees not connected to a high-speed tree, only the

difference in serving costs between high-speed and low-speed service is counted. The disregarded cost, which is the serving cost for all trees when served with high-speed, is incurred by any solution for the Tree Combination Problem. The total cost of a solution to the Tree Combination Problem is this disregarded cost, whose value is a fixed amount C , plus the connection cost and penalties. For the optimal solution to the Tree Combination Problem, the cost can be divided into the fixed cost C and the cost of an optimal solution to the Prize Collecting Steiner Tree problem. Therefore, an α -approximation algorithm for the Prize Collecting Steiner Tree Problem provides an α -approximation algorithm for the original Tree Combination Problem. \square

We use the following known result for the Prize Collecting Steiner Tree Problem

Lemma 4.8 (Archer et al. [1]). *There exists a 1.9672-approximation algorithm for the Prize Collecting Steiner Tree Problem.*

By combining Lemmas 4.4, 4.7 and 4.8, we obtain the following theorem.

Theorem 4.9 (Min-Sum CD with Two Speeds). *There exists an 11.8-approximation algorithm for the non-preemptive Min-Sum CD problem when the drones have only two distinct speeds.*

4.3 Tree Combination Problem with $h \geq 3$ Speeds

When we have drones with more than two speeds, the Prize Collecting Steiner Tree problem cannot be directly applied since the penalty is not fixed before we obtain the final solution. Inspired by the study on the Heterogeneous Traveling Salesman Problem [13], we employ a multi-level primal-dual algorithm to address this issue. If vehicles travel at different speeds and the travel cost is defined as the ratio of the traveled distance to the vehicle's speed, then the travel cost adheres to the principle of monotone costs, which is a prerequisite for the approach to apply.

In the Tree Combination Problem involving multiple-speed drones, we model the solution to include penalties for trees not visited by the highest-speed vehicle. These penalties are assessed at multiple levels, each calculated as the ratio of the distance to the speed difference between consecutive levels.

4.3.1 LP Relaxation and Its Dual

Consider the tree combination problem involving k trees. Later, we will also use vertices to represent each tree. Suppose the k vertices (trees) are ordered according to their respective speeds, and we categorize these vertices into $h \leq k$ distinct levels based on speed. The levels are organized from the fastest to the slowest, with level 1 being the fastest and level h being the slowest. Each level, $l \in [h]$, contains h_l vertices. Formally, let $v_{l,i}$ represent the i -th vertex at speed level l . The set of vertices at level l is denoted as $V_l = \{v_{l,i}\}_{i \in [h_l]}$. For each vertex $v_{l,i}$, where $l \in [h]$ and $i \in [h_l]$, the weight is defined as $w(v_{l,i})$, the subset

of vertices it owns (in the corresponding tree) is $V(v_{l,i})$, and its speed is denoted as p_l .

The input to the tree combination problem is a graph with vertex set $V = \bigcup_l V_l$, edge set $E = \{(u, v) \mid u, v \in \bigcup_{l \in [h]} V_l\}$, where the length of an edge between two nodes $v_{l,i}, v_{l',i'}$ is given by $\ell(v_{l,i}, v_{l',i'}) = \min_{a \in V(v_{l',i'}), b \in V(v_{l,i})} d(a, b)$. A resulting tree rooted at $v_{l,i}$ is defined by $\tilde{T}(l, i) = (\tilde{V}_{l,i}, \tilde{E}_{l,i})$ with $\tilde{V}_{l,i} \subseteq V$ and $\tilde{E}_{l,i} \subseteq E$. The total cost of this tree is equal to the sum of the edge cost $\sum_{(u,v) \in \tilde{E}_{l,i}} \ell(u, v)/p_l$ and the vertex cost $\sum_{v \in \tilde{V}_{l,i}} w(v)/p_l$ if $|\tilde{V}_{l,i}| \geq 1$, and is equal to 0 otherwise. (We set $\tilde{V}_{l,i} = \tilde{E}_{l,i} = \emptyset$ if none of the resulting trees is rooted at $v_{l,i}$.) The objective is to identify a set of trees such that each vertex is included in exactly one of the resulting trees, while minimizing the total cost, i.e.,

$$\sum_{l \in [h], i \in [h_l]} \left(\sum_{(u,v) \in \tilde{E}_{l,i}} \ell(u, v)/p_l + \sum_{v \in \tilde{V}_{l,i}} w(v)/p_l \right).$$

Refer to Figure 2 for an illustration of a tree combination problem involving nine trees across three levels.

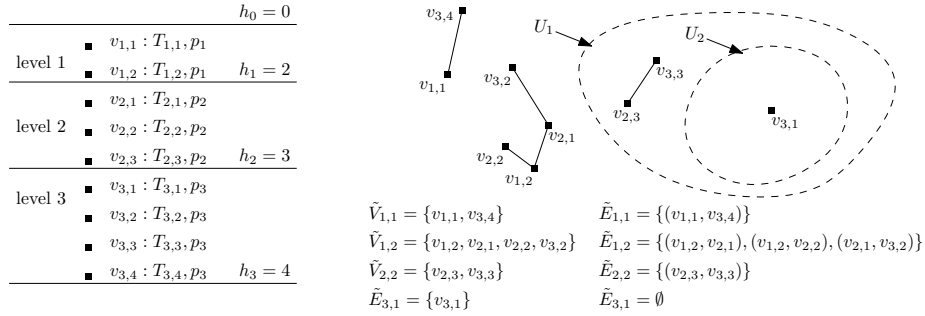


Figure 2: An instance of the tree combination problem with nine vertices, each associated with one of three different speeds $p_1 > p_2 > p_3$. An illustration of a feasible solution shows four resulting trees.

We design an approximation algorithm based on the primal-dual method. To formulate the problem as an integer linear program, we define two sets of integer variables with respect to the following vertex and edge sets:

- The vertex set

$$\bar{V}_l = \bigcup_{l' > l} V_{l'},$$

which consists of vertices that may appear in the resulting trees rooted at a vertex in level l , but are not initially in level l .

- The edge set

$$\bar{E}_l = \{e \in E \mid \text{both endpoints of } e \text{ have level } \geq l\},$$

which consists of edges that may appear in the resulting trees rooted at a vertex in level l .

The two sets of variables are:

- The first set of variables, denoted by x_e^l , indicates whether an edge $e \in \bar{E}_l$ is included in the resulting tree rooted at a vertex in V_l , where $l \in \{1, \dots, h-1\}$.
- The second set of variables, denoted by z_U^l , is defined for $l = 1, \dots, h-1$ and for any subset $U \subseteq \bar{V}_l$. Specifically, $z_U^l = 1$ if U represents the subset of the vertices with speed $p_{l+1}, p_{l+2}, \dots, p_h$ that do not get connected to a vertex with speed p_l or faster.

Let the cost of traversing an edge $e \in \bar{E}_l$ by its root vertex (drone) with speed p_l be denoted by $\text{cost}_l(e) = \ell(e)/p_l$. Denote the cost of serving a vertex v by its root vertex (drone) with speed p_l as $w_l(v) = w(v)/p_l$. Let $\pi_l(U) = \sum_{v \in U} (w_{l+1}(v) - w_l(v))$ be the level- l penalty if all vertices in $U \subseteq \bar{V}_l$ are served by a root vertex with speed less than or equal to p_{l+1} . Notice that if a vertex v is served by a root vertex with speed p_l , then it will be included in the sets U_1, U_2, \dots, U_{l-1} , and the total penalty incurred for this vertex will be $\pi(\{v\}) = \sum_{i=1}^{l-1} \pi_i(\{v\}) = w_l(v) - w_1(v)$. Similar to the tree combination problem with two distinct speeds, we disregard the (positive and fixed) cost of serving all vertices with the highest-speed drone in the integer program, as this does not affect the approximation ratio.

The Integer Programming (IP) formulation and its Linear Programming (LP) relaxation for the problem that we are addressing are as follows:

$$\text{Min} \quad \sum_{l \in [h-1]} \sum_{e \in \bar{E}_l} \text{cost}_l(e) x_e^l + \sum_{l \in [h-1]} \sum_{U \subseteq \bar{V}_l} \pi_l(U) z_U^l \quad (1)$$

$$\text{st.} \quad \sum_{e \in \delta_l(S)} x_e^l \geq \sum_{U: S \subseteq U \subseteq \bar{V}_{l-1}} z_U^{l-1} - \sum_{U: S \subseteq U \subseteq \bar{V}_l} z_U^l \quad \forall S \subseteq \bar{V}_l, l \in [h-1], \quad (2)$$

$$z_V^0 = 1; \quad z_U^0 = 0 \quad \forall U \neq V, \quad (3)$$

$$x_e^l \in \{0, 1\} \quad \forall e \in \bar{E}_l, l \in [h-1], \quad (4)$$

$$z_U^l \in \{0, 1\} \quad \forall U \subseteq \bar{V}_l, l \in [h-1]. \quad (5)$$

Here in constraint (2), we let $\delta_l(S)$ denote the set of edges in \bar{E}_l with exactly one endpoint in S , i.e., $\delta_l(S) = \delta(S) \cap \bar{E}_l$. If we consider solutions where, for each l , $z_U^l = 1$ for exactly one U and $z_U^l = 0$ for all other U , then both terms $\sum_{U: S \subseteq U \subseteq \bar{V}_{l-1}} z_U^{l-1}$ and $\sum_{U: S \subseteq U \subseteq \bar{V}_l} z_U^l$ in constraint (2) only take binary values, either 0 or 1. Then this constraint is trivially satisfied except for the case when $\sum_{U: S \subseteq U \subseteq \bar{V}_{l-1}} z_U^{l-1} = 1$ and $\sum_{U: S \subseteq U \subseteq \bar{V}_l} z_U^l = 0$. But this case can occur only if there is at least one vertex in S that must be connected to a tree rooted at level l . The constraint reduces to $\sum_{e \in \delta_l(S)} x_e^l \geq 1$ in that case and it is ensured that each such vertex is indeed connected to a tree rooted at level l . The IP

formulation also allows solutions in which, for some l , $z_U^l = 1$ for more than one set U , but this cannot increase the objective value of an optimal solution.

The objective is to find a set of resulting trees such that each vertex is included exactly once, and the total cost — including both connection (edge) costs and vertex service costs — is minimized. If a vertex v is connected to a tree rooted at level l , then its cost (penalty) is accounted for in every preceding level from 1 to $l-1$. These costs are included in the penalties associated with the sets U_1, U_2, \dots, U_{l-1} . Specifically, as already mentioned earlier, the cumulative difference in cost for vertex v from level l down to level 1 is given by:

$$w_l(v) - w_1(v) = \sum_{j \in [l-1]} (w_{l+1}(v) - w_l(v)) = \sum_{j \in [l-1]} \pi_j(\{v\}).$$

If we replace the integrality conditions $x_e^l \in \{0, 1\}$ and $z_U^l \in \{0, 1\}$ with $x_e^l \geq 0$ and $z_U^l \geq 0$ and take the dual of the linear program, we obtain the following:

$$\text{Max} \quad \sum_{S \subseteq \bar{V}_1} Y_1(S) \quad (6)$$

$$\text{st.} \quad \sum_{S \subseteq \bar{V}_l: e \in \delta_l(S)} Y_l(S) \leq \text{cost}_l(e), \quad e \in \bar{E}_l, \forall l \in [h-1], \quad (7)$$

$$\sum_{S: S \subseteq U} Y_l(S) - \sum_{S: S \subseteq U - V_{l+1}} Y_{l+1}(S) \leq \pi_l(U) \quad \forall U \subseteq \bar{V}_l, \forall l \in [h-1], \quad (8)$$

$$Y_l(S) \geq 0 \quad \forall S \subseteq \bar{V}_l, l \in [h-1]. \quad (9)$$

The constraints specified in Equation (7) pertain to edges, whereas those in Equation (8) are related to sets of vertices. These constraints limit the dual values assigned to any subset of the set U at each level, ensuring that the combined sum of accumulated values from a higher cost level does not exceed the benefits derived from serving them at the lower cost level.

4.3.2 Primal-Dual Algorithm

Before presenting the algorithm, we first introduce some notation regarding the constraints.

Definition 4.10 (Remaining Potential). *For a given set of vertices $U \subseteq \bar{V}_l$ and a dual feasible solution $Y_l(U)$, we say that $P(Y_l(U), \pi) = \pi_l(U) - (\sum_{S: S \subseteq U} Y_l(S) - \sum_{S: S \subseteq U - V_{l+1}} Y_{l+1}(S))$ is the remaining potential of the set U in l -th level.*

The algorithm maintains a separate forest for each level: The forest of a level consists of trees rooted at vertices within that level to which vertices from higher levels are connected, and possibly some trees that consist only of vertices from higher levels. This organization is achieved through the application of the primal-dual moat-growing procedure, which is implemented independently and

simultaneously across each level's graphs. We define $F_l(t)$ to be the resulting forest at level $l \in [h]$ in the graph $(V_l \cup \bar{V}_l, \bar{E}_l)$ by the end of iteration t of the main loop. For any two levels l and l' , where $l < l'$, and at any iteration t , consider a component C_i in forest $F_l(t)$ and C_j in forest $F_{l'}(t)$. Then C_i is considered an ancestor of C_j , and C_j a descendant of C_i , if $C_i \supseteq C_j$.

A component can be classified as either **active**, **inactive**, or **frozen**. A component is considered **active** at the start of an iteration if it consists of higher-level vertices and its dual variable is allowed to increase during the iteration without violating any constraints in the dual problem. A component is deemed **inactive** if it contains a vertex at the corresponding level or if it is a descendant of an inactive component. A component is **frozen** if it has ceased growing due to constraint (8), at which point its remaining potential becomes 0. If a component is inactive or frozen at the start of an iteration, its dual value will not change during that iteration.

When a component becomes frozen, meaning its remaining potential is reduced to zero, it implies that each of its descendants at the next higher level has either already become frozen or has become inactive.

While the dual LP has only variables $Y_l(S)$ for $S \subseteq \bar{V}_l$, $l \in [h-1]$, in our description of the primal-dual algorithm we consider variables $Y_l(S)$ for $S \subseteq V_l \cup \bar{V}_l$, $l \in [h]$ for ease of presentation. The values of the additionally introduced variables are zero at all times.

Initialization Initially, each forest $F_l(0)$ for level $1 \leq l \leq h-1$ at time 0 consists of singleton components, each of which is a vertex of $V_l \cup \bar{V}_l$. The singleton components containing only vertices from higher levels \bar{V}_l are considered active, while any component containing a vertex with the speed p_l is deemed inactive. The dual variables corresponding to all active and inactive components are initialized to zero, for every $l \in [h]$ and $v \in V_l$, we have $Y_{l'}(\{v\}) = 0$ for all $l' \in [l]$.

Main Loop In each iteration of the primal-dual algorithm, the dual variables of all active components in all forests are simultaneously increased by the same amount as much as possible until at least one of the constraints in the dual problem becomes tight. If multiple constraints in both (7) and (8) become tight simultaneously during iteration t , only one constraint, either from (7) or (8), is chosen and processed based on the following procedure:

If constraints in (7) become tight, then a tight constraint corresponding to the vertex with the lowest level (denoted as l) is chosen first. The edge corresponding to the chosen constraint is added to the forest, merging two components (denoted as C_1 and C_2). If both C_1 and C_2 do not contain a vertex with speed p_l , then the merged component remains active. However, if one of the components contains a vertex with speed p_l (say vertex $v_{l,j} \in C_2$), then the merged component and all its active descendants become inactive.

If a constraint in (8) becomes tight (i.e., it risks being violated if the current dual variables continue to grow) for some component, i.e., $P(Y_l(U), \pi) = 0$, then

the corresponding component U in level l is deactivated and becomes frozen.

The main loop of the algorithm terminates when every component in all forests is either inactive or frozen.

Lemma 4.11. *The main loop of the primal-dual algorithm terminates in $\sum_{l \in [h-1]} |V_l| \cdot (2l - 1)$ iterations.*

Proof. At the start of the main loop, the number of components in all the forest is $\sum_{l \in [h-1]} |V_l| \cdot l$ and the number of active component is $\sum_{l \in [h-1]} |V_l| \cdot (l - 1)$. During each iteration of the main loop, the sum of the number of components and the number of active components in all the forests decreases by at least 1 and thus the main loop will require at most $\sum_{l \in [h-1]} |V_l| \cdot (2l - 1)$ iterations. \square

Let the main loop of the primal-dual procedure terminate after t_f iterations. Then, starting from level $l = 1$, the pruning procedure selects a sub-forest \tilde{F}_l of the level l forest F_l such that each tree of \tilde{F}_l is rooted at one of the vertices in V_l and each vertex is connected in exactly one of the resulting sub-forests. Before describing the pruning procedure, we need to define a few terms. The degree of a subgraph C within a graph (tree) T is defined as:

$$|\{(u, v) : u \in C, v \notin C, (u, v) \in T\}|.$$

A subgraph C of a tree T in level l is referred to as a *frozen subgraph* if C is a component that was frozen in level l during some iteration $t \leq t_f$. In other words, its remaining potential $P(Y_l(C), \pi) = 0$. A subgraph $C \subseteq F_l$ of a tree T in level l is called a *pendent-frozen subgraph* if C is a frozen subgraph and its degree is equal to 1. A *maximal pendent-frozen subgraph* is a pendent-frozen subgraph $C \subseteq T$ such that there is no other pendent-frozen subgraph $C_0 \subseteq T$ with $C_0 \supseteq C$. For each vertex $u \in V$, let $C_l(t, u)$ denote the component containing u in level l at the start of iteration t of the main loop. Define $\text{active}_l(t, u)$ as an indicator for whether $C_l(t, u)$ is active:

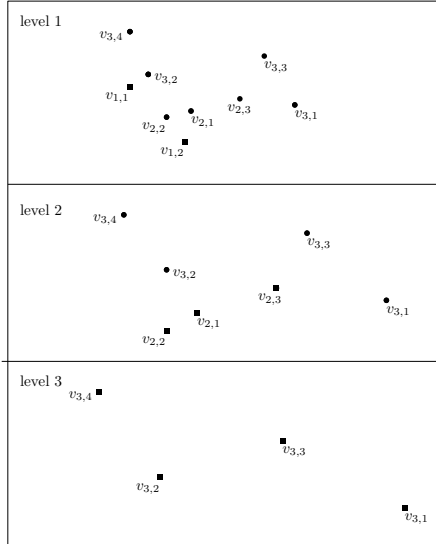
$$\text{active}_l(t, u) = \begin{cases} 1 & \text{if } C_l(t, u) \text{ is active,} \\ 0 & \text{otherwise.} \end{cases}$$

We revisit some observations derived from the execution of the main loop.

Observation 4.12 (Rathinam et al. [13]). *Some observations regarding the primal-dual algorithm:*

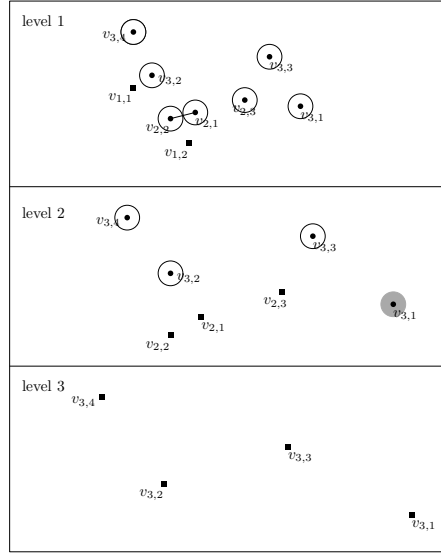
1. *Every component in the Primal-dual procedure is a tree graph.*
2. *Considering edge constraints (7), components at lower levels generally merge earlier than their counterparts at higher levels, primarily because the edge costs between components are smaller at lower levels. For a component containing u in level l , if $l < l'$, then*

$$C_l(t, u) \supseteq C_{l'}(t, u).$$



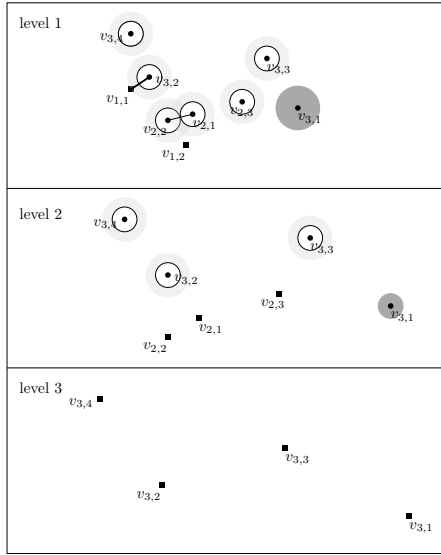
(a) Primal-dual: Initialization

For each level $l \in [3]$, the vertices V_l are inactive and represented by squares, while the other vertices \bar{V}_l are active and represented by disks. In each iteration, all active components' dual variables are increased equally until a dual constraint (either edge constraint or potential constraint) becomes tight.

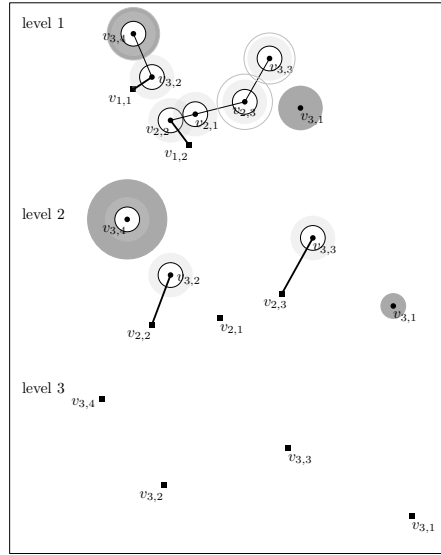


(b) Example of two tight constraints:

Edge constraint: $Y_1(v_{2,1}) + Y_1(v_{2,2}) = \text{cost}_1(\{v_{2,1}, v_{2,2}\})$, thus edge $\{v_{2,1}, v_{2,2}\}$ is added to E_1 , the components $\{v_{2,1}\}$ and $\{v_{2,2}\}$ in level 1 become inactive and the merged component $\{v_{2,1}, v_{2,2}\}$ becomes active. The component $v_{3,1}$ in level 2 becomes frozen.



(c) Edge $\{v_{3,2}, v_{1,1}\}$ is added to E_1 , component $v_{3,1}$ in level 1 becomes frozen.



(d) Final iteration. All components become inactive or frozen.

Figure 3: Illustration of the primal-dual algorithm

3. Regarding vertex constraints (8), components at higher levels tend to freeze before their counterparts at lower levels. This occurs because the corresponding dual value at a higher level ceases to increase, due to one of two reasons: either the component is frozen at all higher levels, or it becomes inactive at a higher level.

Pruning Procedure The pruning procedure is implemented over h iterations. At the start of the pruning procedure, set $l := 1$ and let $F_1 = F_1(t_f)$.

1. From each tree of F_l , remove the maximal pendent-frozen subgraph of F_l and the frozen components from it. The resultant pruned forest is \tilde{F}_l .
2. If $l := h$, stop. Otherwise, let F_{l+1} be the union of discarded pendent-frozen subgraphs and components from F_l in the previous step. Set $l = l + 1$ and go to step 1.

Similar to other primal-dual algorithms, frozen components contain vertices connected to vertices in higher level graphs, and hence the pruning step discards them for processing in an appropriate (higher) levels. Similarly, maximal pendent-frozen subgraphs must be pruned to ensure that no frozen component in this layer contributes a degree of one in the standard degree-based inductive argument for the 2-approximation ratio in the primal-dual method.

Feasibility We first demonstrate that the resulting pruned forests constitute a feasible solution to the Tree Combination Problem. To substantiate this, we show that after any iteration l in the pruning procedure, all vertices $\bigcup_{l' \in [l]} V_{l'}$ from levels $1, 2, \dots, l$ and some vertices of \bar{V}_l are connected to exactly one of the resulting forests $\{\tilde{F}_{l'}\}_{l' \in [l]}$, and the remaining vertices discarded in iteration l are either included in an inactive component or found in frozen components at higher levels.

It is straightforward to verify that this holds true for level $l = 1$, as all vertices are either included in the inactive forest F_1 or contained within some frozen components. Assume that the lemma holds for $l = l'$. We will now demonstrate that the lemma is also valid for $l = l' + 1$. Consider a pruned frozen component C from level l' . For any vertex $u \in C$ at any time t , the component $C_l(t, u)$ is a subset of C and its potential becomes 0 in level l earlier than component C in level l' . This implies that either $C_l(t_f, u)$ is a frozen component in level l and discarded in level l or $C_l(t_f, u)$ is inactive, meaning that $C_l(t, u)$ contains a vertex of V_l . Thus, the components that are pruned away in each pruning step do not affect its connectivity in the higher levels. Hence, the induction step is proved.

Approximation Guarantee We first show that the dual value of the LP relaxation can be equivalently written as the sum of the dual values and penalty costs corresponding to vertices at each level. This will allow us to bound the cost of the edges in the forest of each level with respect to the dual value.

Consider any level $l \in \{1, \dots, h-1\}$. Let \tilde{V}_l denote the set of vertices that are spanned by the forest \tilde{F}_l , and let U_l be the union of the vertex sets $\tilde{V}_{l+1}, \tilde{V}_{l+2}, \dots, \tilde{V}_h$ and $U_0 = V$. We further define X_l to be the set of components not spanned by the resulting forests $\tilde{F}_1, \tilde{F}_2, \dots, \tilde{F}_l$. Notice that the union of the vertex sets of the components in X_l is equal to U_l , since $U_l = \bigcup_{l' > l} \tilde{V}_{l'}$.

We first claim that X_l can be partitioned into sets $X_{l,1}, X_{l,2}, \dots, X_{l,m_l}$ such that $P(Y_l(X_{l,j}), \pi) = 0$ for each set $X_{l,j}$. To see this, note that for any vertex in $X_{l,j}$ either it was connected to a vertex in the level l root set V_l before the deletion process, or it was not. If it was not connected to the root set, then it was in some frozen component I not containing a root vertex, and I was frozen since its potential $P(Y_l(I), \pi) = 0$. If it was connected to a root vertex before the edge deletion process, then it must have been pruned because it is a pendent-frozen subgraph. According to the notation, its remaining potential $P(Y_l(X_{l,j}), \pi) = 0$. Hence, the claim follows.

Lemma 4.13.

$$\sum_{S \subseteq V} Y_1(S) = \sum_{S \subseteq V, S \not\subseteq U_1} Y_1(S) + \sum_{l=2}^{h-1} \sum_{S \subseteq U_{l-1}, S \not\subseteq U_l} Y_l(S) + \sum_{l=1}^{h-1} \pi_l(U_l)$$

Proof. Note that

$$\sum_{S \subseteq V} Y_1(S) = \sum_{S \subseteq V, S \not\subseteq U_1} Y_1(S) + \sum_{S \subseteq U_1} Y_1(S).$$

For any $l = 1, \dots, h-1$,

$$\sum_{S \subseteq U_l} Y_l(S) = \sum_{j=1}^{m_l} \sum_{S \subseteq X_{l,j}} Y_l(S).$$

Since $X_{l,j}$ is a pruned frozen component from level l , therefore its corresponding vertex constraint in (8) is tight. Thus, we have

$$\sum_{S \subseteq U_l} Y_l(S) - \sum_{S \subseteq U_l \setminus V_{l+1}} Y_{l+1}(S) = \pi_l(U_l).$$

Since any component that includes a vertex from V_{l+1} at level $l+1$ becomes inactive and its dual value is 0, it follows that

$$\begin{aligned} \sum_{S \subseteq U_l} Y_l(S) - \sum_{S \subseteq U_l} Y_{l+1}(S) &= \pi_l(U_l). \\ \Rightarrow \sum_{S \subseteq U_l} Y_l(S) &= \sum_{S \subseteq U_{l+1}} Y_{l+1}(S) + \sum_{S \subseteq U_l, S \not\subseteq U_{l+1}} Y_{l+1}(S) + \pi_l(U_l). \end{aligned}$$

Note that $Y_h(S) = 0$ for any subset $S \subseteq V_h$, since all components at level h are singletons and inactive. Applying the above relation recursively, the lemma follows. \square

Similar to the standard degree argument used in the primal-dual algorithm proof for the Prize-collecting Steiner Forest problem [11], for any $l = 1, \dots, h-1$, we have

$$\sum_{e \in \tilde{E}_l} \text{cost}_l(e) \leq 2 \sum_{S \subseteq U_{l-1}, S \not\subseteq U_l} Y_l(S). \quad (10)$$

The approximation ratio will readily follow from these results.

Lemma 4.14. *The primal-dual algorithm constructs a set of forests $\tilde{F}_l = (\tilde{V}_l, \tilde{E}_l)$ such that*

$$\sum_{l \in [h-1]} \sum_{e \in \tilde{E}_l} \text{cost}_l(e) + \sum_{l \in [h-1]} \pi_l(U_l) \leq 2 \sum_{S \subseteq V} Y_1(S)$$

where $U_l = \bigcup_{l' > l} \tilde{V}_{l'}$.

Proof. We now rewrite the cost of the primal solution in terms of the dual variables following Equation (10):

$$\begin{aligned} \sum_{l \in [h-1]} \sum_{e \in \tilde{E}_l} \text{cost}_l(e) + \sum_{l \in [h-1]} \pi_l(U_l) &\leq 2 \sum_{l \in [h-1]} \sum_{S \subseteq U_{l-1}, S \not\subseteq U_l} Y_l(S) + \sum_{l \in [h-1]} \pi_l(U_l) \\ &= 2 \sum_{S \subseteq V} Y_1(S) - 2 \sum_{l \in [h-1]} \pi_l(U_l) + \sum_{l \in [h-1]} \pi_l(U_l) \\ &\leq 2 \sum_{S \subseteq V} Y_1(S) \end{aligned}$$

Note that the second equality follows from Lemma 4.13. \square

Note that the cost of the constructed solution to the Tree Combination Problem equals the cost of the IP solution to the IP obtained via the primal-dual algorithm plus the non-negative fixed cost $\sum_{v \in V} w(v)/p_1$. Therefore, we get a 2-approximation algorithm for the Tree Combination Problem with multiple different speeds. Combining this result with Lemma 4.4, we conclude that there is an 18-approximation algorithm for the non-preemptive Min-Sum CD problem.

Theorem 4.15 (Min-Sum CD). *There exists an $O(1)$ -approximation algorithm for the non-preemptive Min-Sum CD problem.*

5 Algorithmic Adjustments for Implementation

Before presenting the experimental results, we discuss two modifications that we have made in the implementation of our algorithm to improve the performance, both in terms of running time and solution quality, in practical problem settings. First, we refine the algorithm for tree construction (Algorithm 2). A straightforward implementation of step 2 of Algorithm 2 would involve constructing the

graph G' of size $O(n^2)$ and computing an MST in $O(n^2)$ time. In our experiments we only consider instances where all input points lie in the Euclidean plane. Then the MST is a subset of the Delaunay triangulation. We therefore compute a Delaunay triangulation in $O(n \log n)$ time [8] before contracting the depots into a single depot r (referred to as *super-depot* in the remainder of this section). The resulting graph has $O(n)$ edges, and an MST can be computed in $O(n \log n)$ time. This significantly reduces the running time.

Furthermore, we observed in the experiments that computing first an MST of the sources and then attaching the targets produces trees that lead to solutions of relatively large cost. This is because the vehicles move from the target of one request to the source of the next request they serve, and therefore target-to-source distances are more relevant to the application than source-to-source distances. We would therefore like to grow the spanning tree in a Prim-like fashion by adding to the tree the request whose source is closest to the *target* of a request that is already in the tree, rather than the request whose source is closest to a *source* already in the tree. A straightforward implementation of this idea would increase the running-time significantly, however, as after a request is added to the tree, the priority of all sources of requests not yet in the tree may need to be updated. To avoid this computational expense, we use the Delaunay triangulation to determine for each target a (small) set of nearby candidate sources, and we update only the priority of those candidate sources.

As the total length of a spanning tree constructed in this way might not be within a constant factor of the MST of sources (with targets attached) on some pathological input instances, we consider a further modification that guarantees that the spanning tree constructed is within a constant factor of the MST of sources (with targets attached): When deciding which request to add to the tree, we add the request with minimum target-to-source distance d_{ts} only if d_{ts} is at most k times the minimum source-to-source distance d_{ss} between the tree and a request not in the tree, where k is a small constant. This ensures that the spanning tree constructed has total length at most k times the total length of an MST of the sources (and super-depot) with the targets attached. We add ‘MST k ’ in brackets after the name of an algorithm to indicate that this modification has been applied.

Second, we consider three alternatives for converting the large trees produced as solution to the Tree Combination problem by our primal-dual algorithm into tours. In the theoretical analysis, we had constructed the tours as Euler tours of the large trees. In the implementation, we perform a DFS of the large tree and let the vehicle serve the requests in the order in which their sources are first visited by the DFS. The length of a tour constructed in this way is within a constant factor of the total length of the large tree. We refer to the algorithm with this tour construction method as PD-DFS.

As an alternative, we implemented the following cheapest-insertion heuristic: Build the tour for a large tree incrementally. Initially, the tour consists only of the depot of the fastest vehicle. Then process the requests in the large tree in arbitrary order, and insert each request at the position of the tour where it leads to the smallest increase in length (either right after the depot or right after the

target of a request already in the tour). We refer to this method as PD-Greedy. It is efficient as long as the number of requests included in a large tree is not too large.

As a final alternative, we implemented a two-stage version of the cheapest-insertion heuristic: First, use the cheapest-insertion heuristic to build a tour for each of the original trees included in the large tree. Then, use the cheapest insertion heuristic again to produce an order of the tours produced for the original trees (discarding their depots), starting with the tour of the original tree of the fastest depot. We refer to this method as PD-DGreedy (“double-greedy”).

We note that PD-DFS (MST k) is guaranteed to produce a solution that is a constant-factor approximation of the optimal solution, while the other algorithm variants do not guarantee this property for all inputs.

In the following, we describe the above-mentioned adjustments in full detail.

Adjustment 1: Minimum-Cost Tree Construction The tree construction algorithm (Algorithm 2) is adjusted as follows: We build the tree in a Prim-like fashion. We allow each (s, t) pair also to be connected to the destination of another package in the tree rather than only to the super-depot or a source that is already in the tree. The packages that are not yet in the tree are maintained in a priority queue, and the priority of a package (s, t) in the priority queue is the minimum distance between s to the super depot or any destination already in the tree. If the MST k modification is used, the minimum distance between s and a source already contained in the tree, multiplied with factor k , is also included in the computation of the priority. At any time, the package with minimum priority is then removed from the priority queue and added to the tree. A straightforward implementation of this idea would cause the running time to increase substantially, however, as adding one (s, t) pair to the tree could require the priority of all remaining packages in the priority queue to be updated. To circumvent this, we determine a set of *candidate sources* for each destination as follows. Assuming that the input points are points in the Euclidean plane, we first compute a Delaunay triangulation [8] of the sources. For each destination, we then determine a small set of candidate sources that are ‘near’ the destination, as determined via the Delaunay triangulation. When an (s, t) -pair gets added to the tree, we then only update the distances of the candidate sources of t , leading to a significantly reduced running time. (If the MST k modification is used, we also update the Delaunay neighbors of s .)

Step 1: Super-depot contraction. All depots are contracted into a virtual node r_{super} , the super depot. For each source node, its distance to r_{super} is defined as the distance to the nearest depot.

Step 2: Source-only Delaunay triangulation¹. A Delaunay triangulation is

¹We also experimented with constructing a target-only Delaunay triangulation (and using it to determine for each source the targets to which it is near), allowing each source to have one or more opportunities for its connection cost to be updated. However, in tests with uniformly

constructed using only the source nodes, producing a sparse set of edges among them.

Step 3: Determine candidate sources (see Figure 4). For each target node t :

Step 3.1: If t lies inside the circumcircle of any Delaunay triangle, the corresponding triangle is considered relevant to t and its three vertices are added to the set of candidate sources for t .

Step 3.2: If t does not lie inside any circumcircle, two tangent lines are drawn from t to the convex hull of the sources. The chain of hull vertices between the tangent points is taken as the candidate source set.

Step 3.3: If the source s corresponding to t (i.e., the source s of the package that is to be delivered to t) is contained in the candidate source set, then all neighbors of s in the Delaunay graph are also added to the set.

Step 4: Prim-based tree construction. A Prim-like algorithm is executed on the sparse graph consisting of r_{super} , the sources S , and the targets T :

Step 4.1: The connection cost of each source is initialized as its distance to r_{super} (Step 1).

Step 4.2: The source with the minimum connection cost is selected and connected to the tree.

Step 4.3: The paired target t of the selected source is immediately connected.

Step 4.4: (a) The connection costs of the candidate sources associated with this target (Step 3) are updated. More precisely, for every candidate source s that is not yet in the tree and has current priority p , its priority is updated to $\min\{p, d(t, s)\}$.

(b) If the MST k modification is used: The connection costs of all Delaunay neighbors of the source selected in Step 4.2 are updated. Specifically, for every source s' that is not yet in the tree and is a Delaunay neighbor of the selected source s^* , if its current priority is p' , then its priority is updated to $\min\{p', k \cdot d(s^*, s')\}$, where k is a fixed constant.

Step 4.5: Steps 4.2–4.4 are repeated until all (s, t) pairs are connected into the tree.

Step 5: Super-depot expansion. The virtual node r_{super} is replaced by the original depots.

Step 6: Return the collection of trees obtained.

distributed points, this approach produced higher final costs compared to the source-only Delaunay method.

Steps 2 and 3 play a critical role in reducing the computational burden: once a new (s, t) pair is connected, only the sources in the vicinity of the corresponding target, and potentially the sources that are Delaunay neighbors of s , require cost updates, rather than all sources.

Step 4.4 can be instantiated in two ways. The first variant applies only rule (a) and updates connection costs solely via target to source distances. This variant follows the problem structure by prioritizing target-to-source connections, but it does not guarantee a constant approximation ratio. In particular, a subtle difficulty arises when certain sources are distant from all targets: In such cases, the connection costs of these sources may not be updated during the process and thus remain at their initial values, defined as the distance to the virtual super-depot r_{super} . The second variant, called the MST k modification, applies both rules (a) and (b). In this case, we maintain two priorities for each remaining source: (i) its best source–target priority P_{ST} (the minimum distance from targets currently in the tree, initialized as the distance from the super-depot), and (ii) its best source–source priority P_{SS} (to the sources that are Delaunay neighbors). If $P_{ST} \leq k \cdot P_{SS}$, we add the request corresponding to P_{ST} ; otherwise, we add the request indicated by P_{SS} . Here, k is a fixed constant. This additional consideration of source–source distances is essential for guaranteeing a constant-factor approximation ratio.

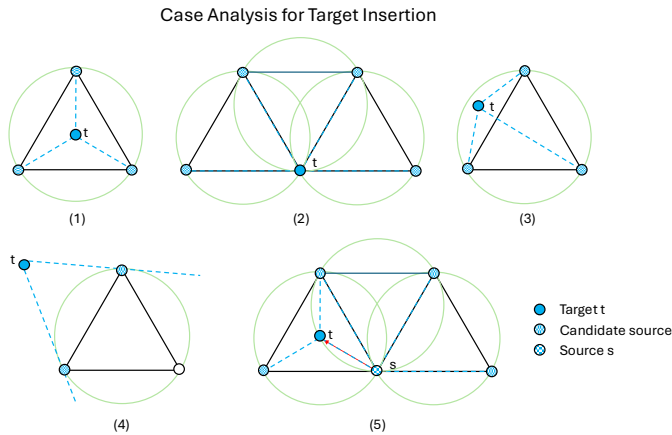


Figure 4: The cases for determining candidate sources: (1)–(3) Step 3.1: The target t lies inside the circumcircle of any Delaunay triangle. (4) Step 3.2: The target t lies outside all circumcircles. (5) Step 3.3 : The corresponding source s of t is contained in the candidate source set.

Adjustment 2: Heuristic Final Path Construction The result of the primal-dual procedure is a set of large trees, each of which is a combination of one or several original trees. We refer to the original trees also as *small trees* in the following. Each of the small trees is associated with a depot, and for each large tree we assign the fastest depot (vehicle) of its small trees to serve all (s, t)

pairs in the large tree.

We consider three different methods for constructing the final tour for each large tree. Based on the approach used in the proof of Lemma 4.4, our first method is to perform a depth-first search (DFS) traversal on each large tree to construct a feasible final path. This procedure is computationally efficient, and the total cost of the resulting path is within a constant factor of the tree cost, providing the desired performance guarantee. We refer to this implementation as the *Primal–Dual Algorithm with DFS* (PD-DFS).

The second method is to use the greedy cheapest-insertion heuristic: For each large tree, we construct a route for its fastest vehicle to serve all requests in the large tree. As this is done separately for each large tree, the need to compare against different depot paths and possible insertion positions is eliminated. This substantially reduces the computational cost and explains why our algorithm performs significantly faster than the heuristic baseline (see Section 6). We refer to this approach as the *Primal–Dual Algorithm with Greedy Routing* (PD-Greedy).

Additional efficiency is achieved by exploiting the fact that the requests in a large tree are partitioned among the small trees that make up the large tree. Specifically, we first apply the cheapest-insertion heuristic separately to the set of packages in each small tree (starting with the depot that was originally associated with that small tree). We then apply the heuristic a second time to determine the order in which the resulting paths (starting with the path of the small tree that contains the depot with the fastest drone, and omitting the depots of the paths of all other small trees) are combined into the final path. If both the number of packages in each small tree and the number of small trees within each large tree are small, the greedy cheapest-insertion heuristic is applied only to instances of small size, resulting in a reduced running time. We refer to this approach as the *Primal–Dual Algorithm with Double Greedy Routing* (PD-DGreedy).

By adjusting the tree construction procedure and considering three different methods for final path construction, we thus have three variants of our PD-based algorithm:

- *Primal–Dual algorithm with Depth-First Search Routing* (PD-DFS);
- *Primal–Dual algorithm with Greedy Routing* (PD-Greedy);
- *Primal–Dual algorithm with Double Greedy Routing* (PD-DGreedy).

Furthermore, for each of these algorithms we can optionally apply the MST k modification to the tree construction step. In our experiments we found that the choice $k = 7$ worked best, and we refer to these three variants as PD-DFS (MST 7), PD-Greedy (MST 7), and PD-DGreedy (MST 7).

Running Time Analysis For ease of presentation of the following analysis, we make the natural assumption that $k \leq n$. In the tree-construction phase, we first construct a Delaunay triangulation of the source nodes. This step runs in

$O(n \log n)$ time [8]. We then determine for each target node a set of candidate sources; this also takes $O(n \log n)$ time provided that the number of candidate sources for each target node is constant on average, which is typically the case. The Prim-based construction of a spanning tree then also runs in $O(n \log n)$ time.

In our implementation of the primal-dual procedure, as analyzed in Lemma 4.11, the main loop of the algorithm terminates after $\sum_{l \in [h-1]} |V_l| \cdot (2l-1)$ iterations, where V_l denotes the set of constructed trees whose depots are at level l . Note that $|V_l| \leq k$. The number of iterations of the primal-dual procedure thus depends only on k and h , independent of the number of requests.

When the number of request pairs is small, the primal-dual phase dominates the running time. When the number of request pairs is large, the computation of the final routes becomes more computationally expensive, especially for PD-Greedy and PD-DGreedy. Specifically, the routing part of the PD-DFS algorithm requires $O(\sum_i N_i) = O(n)$ time, where N_i denotes the number of source-target pairs contained in the i -th large tree produced by the primal-dual algorithm. The routing part of the PD-Greedy algorithm requires $O(\sum_i N_i^2)$ time, where N_i denotes the number of source-target pairs contained in the i -th large tree produced by the primal-dual algorithm. The routing part of the PD-DGreedy algorithm requires $O\left(\sum_i \left(S_i^2 + \sum_j M_{i,j}^2\right)\right)$ time, where S_i denotes the number of small trees contained in the i -th large tree and $M_{i,j}$ denotes the number of source-target pairs in the j -th small tree contained in the i -th large tree.

The algorithmic adjustments discussed in this section partly improve the running time and partly improve the solution quality at the cost of a small increase in running time. In the next section, we evaluate the performance and running time of our PD-based algorithms relative to a baseline algorithm.

6 Computational Experiments

In Section 6.1, we describe the synthetic and real-word instances used for our experiments as well as the baseline algorithm to which we compare our primal-dual based algorithms. Then, in Section 6.2, we present the results of our experiments. Our implementations, which allow all experimental results to be fully reproduced, are publicly available at https://github.com/WenZhang-Vivien/Tree_construction_Primal_Dual_Routing

6.1 Instances and Baseline Algorithm

Synthetic Datasets We consider three synthetic datasets in our experimental evaluation. The first dataset is constructed based on the worst-case instance described below for the baseline algorithm with which we compare the performance of our algorithms. It is used to demonstrate the guaranteed performance of our algorithms relative to the baseline.

The second dataset, denoted by SY-U, consists of instances in which all locations—including request pickup locations, drop-off locations, and depot locations—are independently generated from a uniform distribution over a $[0, 100] \times [0, 100]$ grid.

The third dataset, denoted by SY-GMM, is generated using a Gaussian mixture model with c clusters. Each cluster follows a bivariate Gaussian distribution whose center is sampled uniformly from the $[0, 100] \times [0, 100]$ grid and whose covariance matrix is given by $\sigma^2 I$. To study the effects of clustering structure and spatial dispersion, we evaluate multiple combinations of the parameters c and σ , as summarized in Table 1.

Table 1: Parameter settings for the synthetic datasets. Bold values indicate fixed parameters used in the sensitivity analyses, while “–” denotes parameters that are not applicable.

Parameter	Worst-case	SY-U / SY-GMM
n (number of requests)	5, 10, 15, 20 ($\times 10^3$)	5, 10 , 15, 20 ($\times 10^3$)
k (number of depots)	2	1, 3, 5, 7, 9, 10, 15, 20, 30 , 40 ($\times 3$)
h (number of speeds/levels)	2	1, 2, 3 , 4, 5
c (number of clusters)	–	– / 1, 2, 3, 4, 5, 6 ($\times 5$)
σ (cluster covariance)	–	– / 1, 2, 3, 4, 5, 6 ($\times 5$)

Realworld Datasets We also conduct experiments using a real-world dataset collected from Meituan [12], one of the largest on-demand delivery platforms. The dataset contains orders, couriers (we treat the initial locations of the couriers as depots), and delivery records from an anonymized midsize city in China. To capture both regular and peak demand patterns, we select one representative weekday (October 18, 2022) and one representative weekend day (October 22, 2022) for evaluation.

To study scalability under varying system sizes, we consider multiple depot-scale settings with 3, 9, 15, 21, 27, 30, 45, 60, 90, and 120 depots. For each setting, depots are randomly sampled from the full pool of available depots. To ensure controlled comparisons across different scales, depot sets are constructed incrementally: the depot set in a larger-scale setting strictly contains the depot set from the previous smaller-scale setting. For example, the 15-depot configuration includes the same three depots used in the 3-depot setting, together with 12 additional depots randomly sampled from the remaining depots.

For each depot configuration and each selected day, all orders recorded on that day in the dataset are used as requests. In these datasets, each location is represented by its latitude and longitude coordinates. The distance between two locations is defined as the Euclidean distance between their coordinates. A summary of key statistics for all experimental settings, including the number of depots, number of orders, and other relevant characteristics, is reported in Table 2.

Table 2: Parameter settings for the real-world datasets.

Parameter	Weekday	Weekend
n (number of requests)	69,103	77,638
k (number of depots)	1, 3, 5, 7, 9, 10, 15, 20, 30, 40 ($\times 3$)	
h (number of speed levels)		3

Baseline Algorithm We are not aware of any previously proposed methods for the heterogeneous collaborative delivery problem. Heuristic algorithms, such as greedy methods, tend to be computationally efficient and align well with our goal of solving the problem quickly. Therefore, we consider the following cheapest-insertion heuristic algorithm as the baseline in our experiments. The algorithm begins with an arbitrary order of requests and processes them sequentially. For each request, it evaluates all vehicles and all insertion positions within their current routes (a request can be inserted after the depot or after the destination of any package that is already contained in the route), computing the additional travel time incurred. The request is then assigned to the vehicle and insertion position that yields the minimum increase in cost. This process is repeated until all requests are placed, producing a feasible set of routes that serves as a baseline for comparison in our experiments. The running time of the baseline algorithm is $O(n(k+n))$.

We emphasize that this greedy cheapest-insertion heuristic is not a constant-factor approximation, even in the special case where each request is of the form $s_i = t_i$. In fact, we next construct an instance where the algorithm incurs a cost $\Theta(\alpha)$ times the optimal solution, where $\alpha = v_{\max}/v_{\min}$ is the ratio of the maximum to minimum vehicle speed.

Worst-case Instance of the Baseline Algorithm Consider two vehicles with speeds v_1 and $v_2 = \alpha v_1$ with $\alpha > 1$, located at distinct depots o_1 and o_2 respectively. There are n requests $\{(s_i, t_i)\}_{i=1}^n$ with $s_i = t_i$. The depots and request endpoints are placed in a line metric as follows:

- o_1 is placed at $-nv_1$,
- o_2 is placed at $-(n+\varepsilon)v_2$ for some small $\varepsilon > 0$,
- $s_i = t_i$ is placed at $(i-1)nv_1$ for $i = 1, 2, \dots, n$.

By construction, the greedy cheapest-insertion heuristic assigns all requests to the slower vehicle (vehicle 1). Hence, the total travel time is

$$\frac{n \cdot n \cdot v_1}{v_1} = n^2.$$

On the other hand, if all requests are served by the faster vehicle (vehicle 2), then the total travel time is

$$\frac{(n+\varepsilon) \cdot v_2 + (n-1) \cdot n \cdot v_1}{v_2} \leq n + \varepsilon + n^2 \cdot \frac{v_1}{v_2}.$$

When n is large, the optimal solution cost approaches $O(n^2 \cdot \frac{v_1}{v_2})$, whereas the greedy algorithm incurs cost n^2 . Thus, the approximation ratio of the greedy heuristic is $\Theta(v_2/v_1) = \Theta(\alpha)$, showing that the algorithm is not a constant-factor approximation.

6.2 Experimental Evaluation

We first present the results for synthetic inputs and then those for real-world data.

6.2.1 Computational Results in Synthetic Data Sets

In this section, we present the results on the worst-case, SY-U, and SY-GMM datasets. For the total travel time objective, the baseline algorithm performs well in synthetic data sets, but is slowest, and in some instances can perform significantly worse due to the lack of a performance guarantee. All three PD-based algorithms run faster than the baseline algorithm. Among them, PD-Greedy consistently achieves performance close to that of the baseline algorithm. PD-DFS is the fastest algorithm, but its solution quality in the experiments is worse than that of the other two. PD-DGreedy offers a good trade-off: it is faster than PD-Greedy while achieving better performance than PD-DFS.

Computational Results in Worst-Case Data Sets We construct a worst-case dataset on a line metric with two speed levels, following the example described in the previous section. Specifically, we set ε , v_{\max} , and v_{\min} as fixed parameters and increase the number of source–target pairs n . We let $\alpha = v_{\max}/v_{\min} = 1,000$. Figure 5 shows the solution cost and running-time versus the number n of requests. As n increases, the total cost of the baseline algorithm grows with n^2 whereas the costs of all PD-based algorithms are about 1,000 times smaller, demonstrating the superior performance of our proposed methods. The MST 7 variants of the PD algorithms produce the same solutions as the variants not using the MST 7 modification and are not shown.

In terms of running time, all algorithms except PD-DFS exhibit significant increases in running time as the number of requests n increases. The baseline algorithm consistently requires more running time than the PD-based algorithms across all instances. Compared to the other algorithms, the running time of PD-DFS grows much more slowly as the number of requests increases.

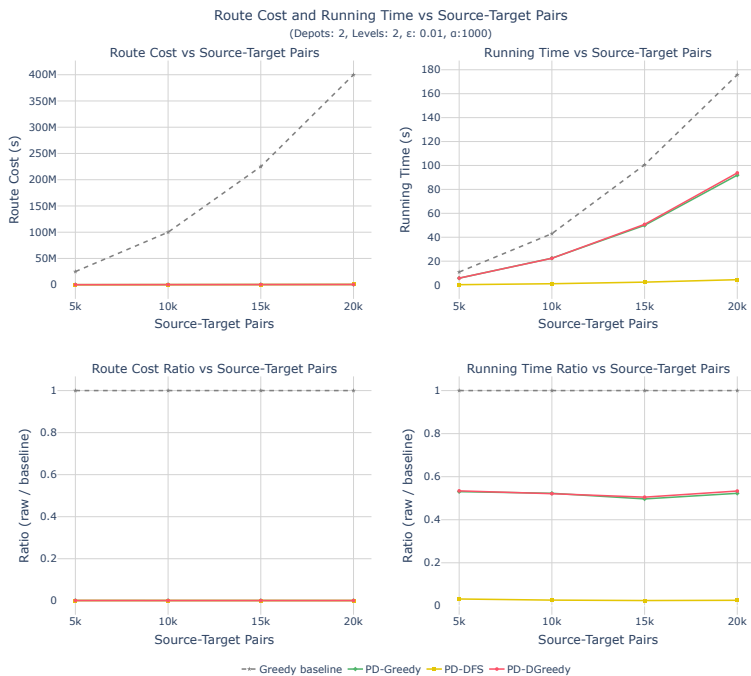


Figure 5: Results on the worst-case instance for the baseline algorithm with varying n , where $\alpha = v_{\max}/v_{\min}$ and ϵ is a small constant parameter (see Section 6.1).

Computational Results in SY-U and SY-GMM Data Set Figures 6, 8, and 10 illustrate the impact of the number of source–target pairs n , the number of depots k , and the number of speeds/levels h on algorithm performance for data generated from a uniform distribution. The corresponding figures for data generated from a GMM distribution can be found in Appendix A. We observe that the performance trends on the SY-GMM datasets are similar to those on the SY-U datasets; therefore, we only provide a detailed discussion of the effects of n , k , and h for the uniform case. Finally, we examine how the performance and running time vary with respect to the GMM parameters, namely the number of clusters c and the cluster covariance σ .

For a fixed number of depots ($k = 90$) and a fixed number of speed levels ($h = 3$), as the number of source–target pairs n increases from 5×10^3 to 20×10^3 as shown in Figure 6, the ratio between the total travel time objective of our PD-Greedy (and PD-DGreedy) algorithm and that of the baseline algorithm decreases and approaches 1. Meanwhile, the ratio of the running times remains below 1 and continues to decrease, indicating a growing computational advantage of our approach at larger scales. The MST 7 variants of the PD algorithms tend to produce slightly better solutions at the expense of a slightly increased

running time.

Figure 7 illustrates the breakdown of the running time of the individual components of each PD-based algorithm as the number of request pairs increases. When n is small (e.g., $n = 5,000$), the primal-dual component dominates the running time. As n increases, the routing phases account for a larger portion of the total running time: first the PD-Greedy routing component becomes dominant (around $n = 10,000$), followed by the PD-DGreedy routing component (around $n = 15,000$), and for sufficiently large n (e.g., $n = 20,000$), the PD-DFS routing phase also dominates the primal-dual step.

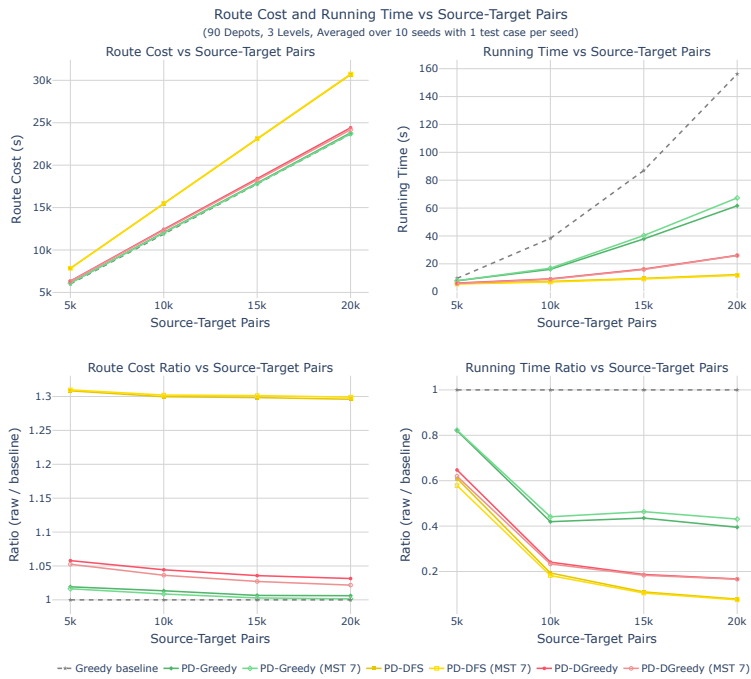


Figure 6: Results on the Uniform synthetic dataset (SY-U) with varying n .

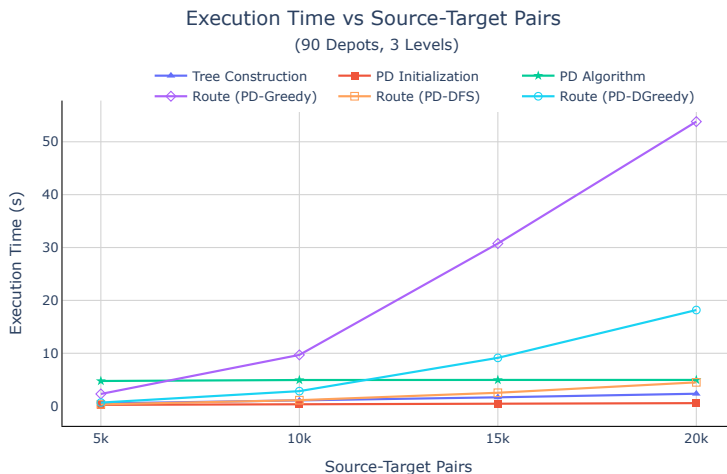


Figure 7: Breakdown of running time for the three PD-based algorithms on the Uniform synthetic dataset (SY-U) with varying n .

For a fixed number of source-target pairs ($n = 10 \times 10^3$) and a fixed number of speed levels ($h = 3$), when the number of depots k is small (less than 30), as shown in Figure 8, our PD-Greedy (and PD-DGreedy) algorithm outperforms the baseline in terms of solution quality; with an increasing number of depots, the baseline algorithm attains slightly better performance. In terms of running time, the PD-based algorithms are always faster than the baseline. Interestingly, the running time of all PD-based algorithms decreases as the number of depots increases when the number of depots is relatively small (less than 60), and then increases thereafter. This behavior can be explained by the changing dominance of different algorithmic components. When the number of depots is small, the routing component dominates the overall running time, and its cost decreases as more depots are added. As the number of depots becomes large, the primal-dual (PD) component becomes dominant, leading to increased running time with further increases in the number of depots. This trend is illustrated in Figure 9, where we separately report the running times of the individual components of each PD-based algorithm as the number of depots varies. These observations suggest that, for a fixed number of source-target pairs, there may exist an appropriate number of depots that simultaneously yields best solution quality and fast running time.

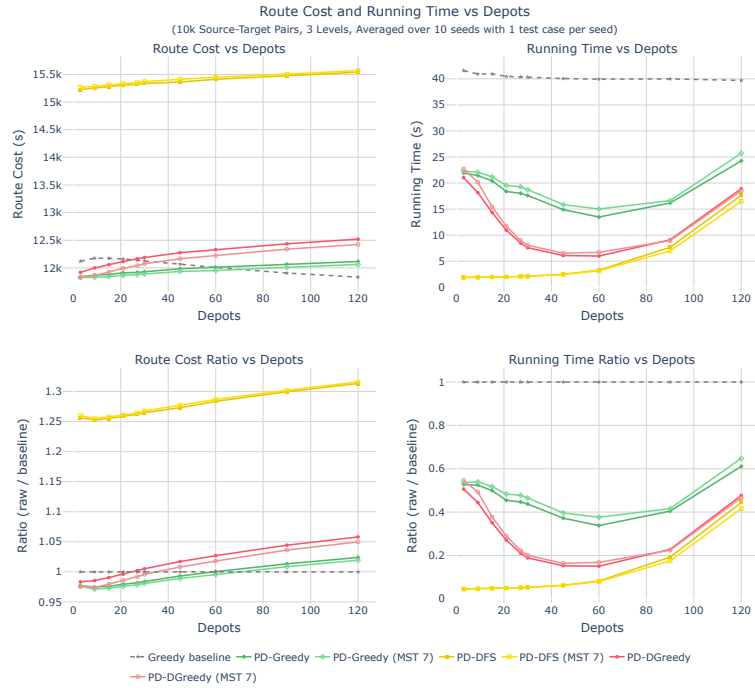


Figure 8: Results on the Uniform synthetic dataset (SY-U) with varying k .

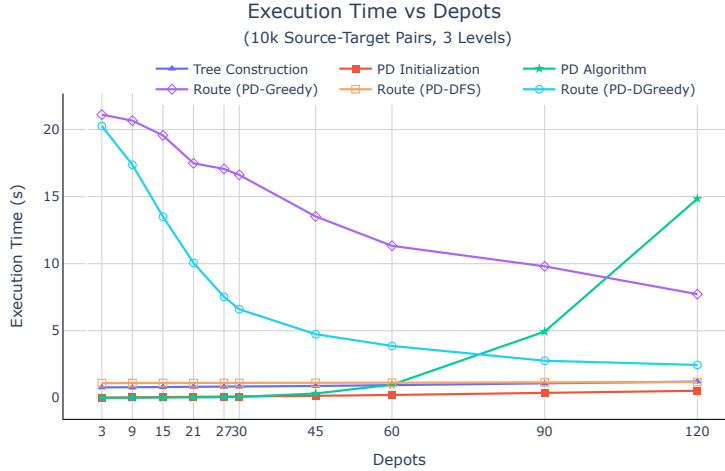


Figure 9: Breakdown of running time for the three PD-based algorithms on the Uniform synthetic dataset (SY-U) with varying k .

For a fixed number of source-target pairs ($n = 10 \times 10^3$) and a fixed number of depots ($k = 90$), as the number of speed levels h increases, as shown in Figure 10, the performance of our PD-Greedy algorithm is slightly worse than that of the baseline algorithm when the number of speed levels is small (less than 3), but becomes superior as the number of speed levels increases. In terms of running time, the baseline algorithm spends most of its time in the same computational components, and its running time therefore remains largely unchanged as the number of speed levels increases. In contrast, the running time of our PD-based algorithms increases with the number of speed levels, but they consistently remain faster than the baseline algorithm. This increase is mainly due to the Primal Dual component, whose running time grows with the number of speed levels. This trend is illustrated in Figure 11, where we separately report the running times of the individual components of each PD-based algorithm as the number of speed levels varies.

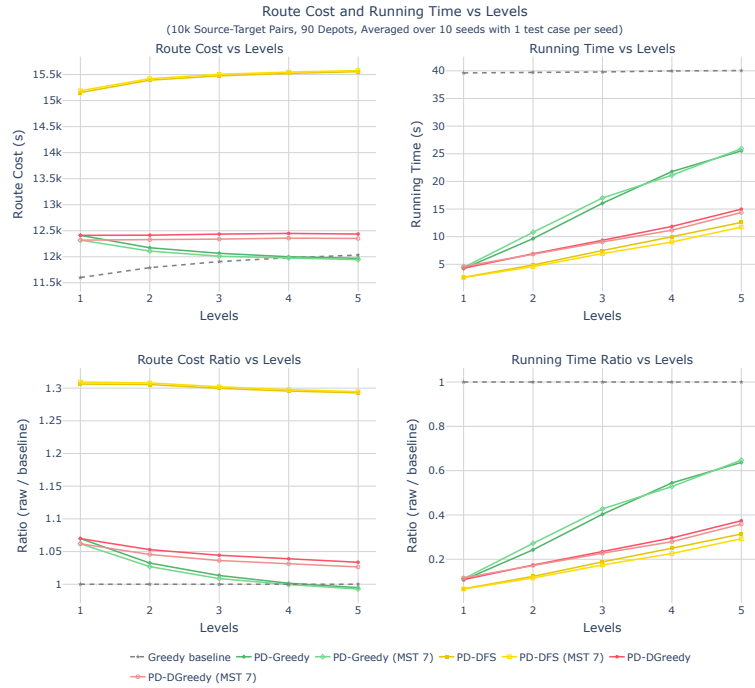


Figure 10: Results on the Uniform synthetic dataset (SY-U) with varying h .

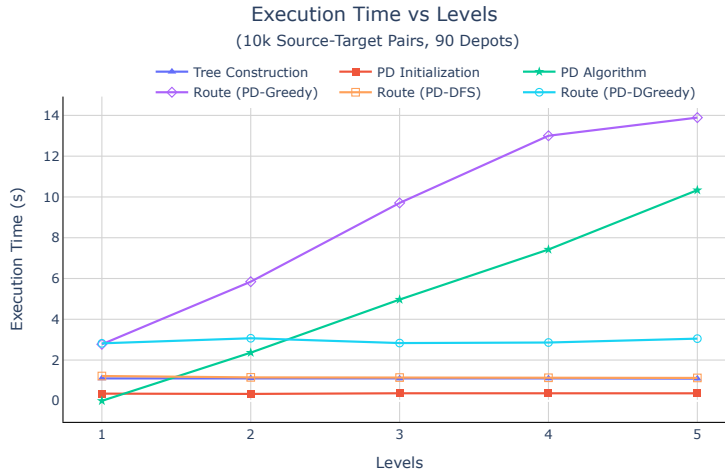


Figure 11: Breakdown of running time for the three PD-based algorithms on the Uniform synthetic dataset (SY-U) with varying h .

Figure 12 illustrates the effect of the GMM distribution parameters—the number of clusters c and the covariance σ —on algorithm performance. All three PD-based algorithms exhibit similar trends, with PD-DFS (yellow curve) clearly illustrating the performance changes with respect to c and σ in the figure.

As either c (which partitions source-target pairs into more spatially separated clusters) or σ (which increases spatial variance) grows, the data become more spatially dispersed. In this setting, the greedy cheapest-insertion heuristic performs poorly because local cost minimization leads to early routing decisions that create large and irreversible inter-cluster detours. In contrast, the PD-based algorithms leverage early assignment and hierarchical structure to better respect the spatial organization of the data, resulting in increasingly lower route cost ratios and a growing performance advantage over the greedy baseline.

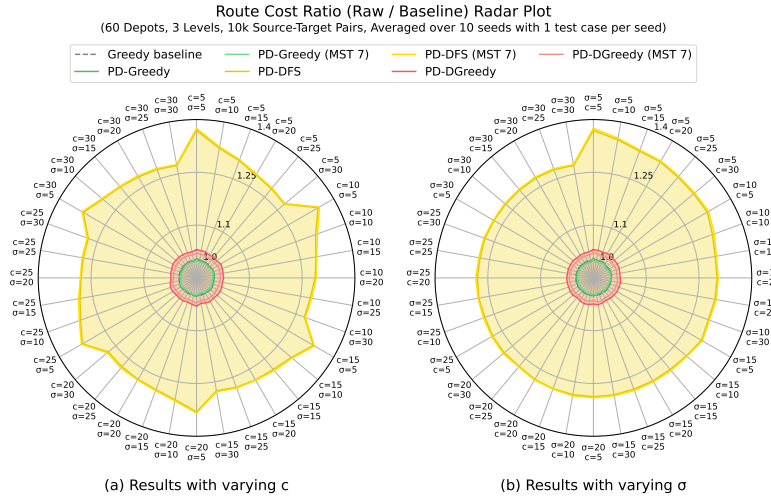


Figure 12: Results on the GMM synthetic dataset: varying c and σ .

Computational Results in Realworld Data As observed in the synthetic datasets, a relatively small number of depots (vehicles) is sufficient to achieve good performance with low running time. Accordingly, we focus on representative settings with different numbers of depots k , selected at random, and compare the performance of the three PD-based algorithms against the baseline algorithm on both weekday and weekend real-world data, considering both the full set of depots (only for the baseline algorithm) and randomly selected depot subsets.

From Figure 13 (weekday data) and Figure 14 (weekend data), we observe trends consistent with those seen in the synthetic experiments. First, PD-Greedy achieves the best solution quality, while PD-DFS is the fastest among the PD-based methods. Second, as the number of depots increases, the total route cost of the PD-based algorithms—particularly PD-greedy and PD-DGreedy—slightly increases from their initially strong performance; however, their cost remains consistently low relative to the baseline, with a ratio no greater than 1.1. Meanwhile, the running time of the PD-Greedy and PD-DGreedy algorithms continues to decrease as more depots are included, due to the reduced number of packages assigned to each depot. This trend becomes more pronounced for large-scale real-world source-target request pairs.

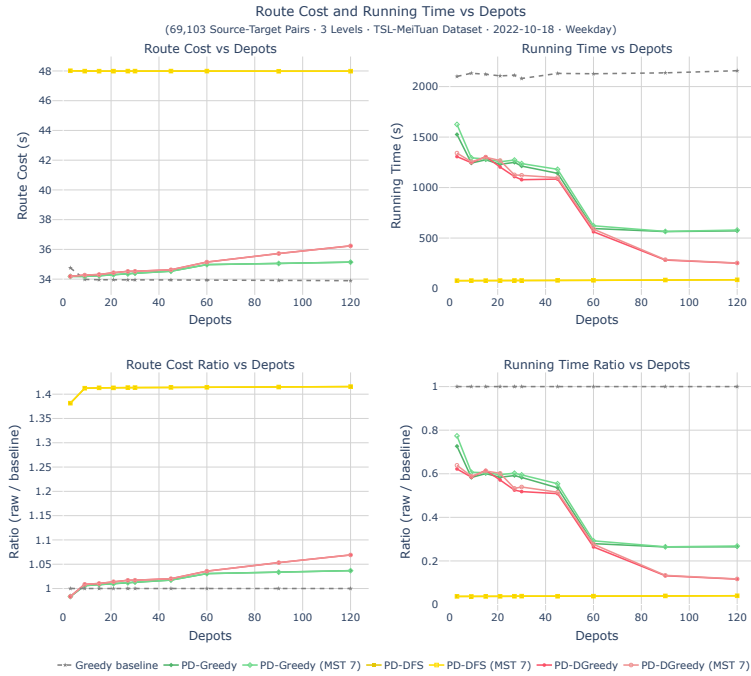


Figure 13: Results on the weekday dataset with varying numbers of depots k . We compare the PD-based algorithms with the baseline algorithm using the same randomly selected depot sets. For reference, when the baseline algorithm uses all depots, the total route cost is 32.066 seconds and the running time is 2137.99 seconds.

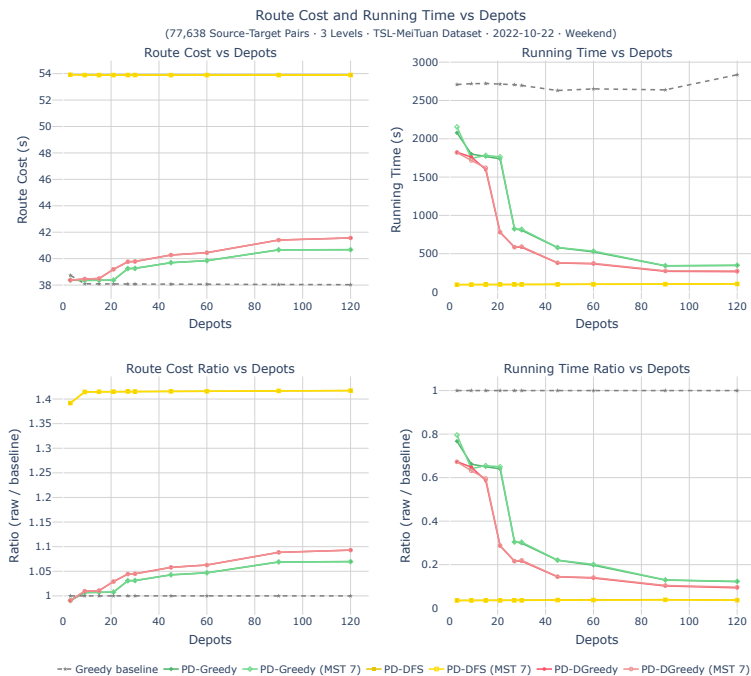


Figure 14: Results on the weekend dataset with varying numbers of depots k . We compare the PD-based algorithms with the baseline algorithm using the same randomly selected depot sets. For reference, when the baseline algorithm uses all depots, the total route cost is 36.12 seconds and the running time is 2731.58 seconds.

We remark that, for both the synthetic datasets and the real-world datasets, the effects of varying n , k , and h exhibit similar trends. As the number of request pairs increases, our algorithm continues to achieve favorable performance, particularly when fewer depots are used, while maintaining relatively low running times.

7 Conclusion

In this paper, we extend the study of multi-package collaborative delivery to the speed-heterogeneous setting and provide new theoretical insights and practical algorithmic approaches. We show that the benefit of fine-grained collaboration over coarse-grained collaboration is limited and devise a primal-dual based constant-factor approximation algorithm for minimizing the total travel time with coarse-grained collaboration. Furthermore, we propose several algorithmic adjustments to improve the performance of the algorithm in practical settings,

both in terms of running time and solution quality. In experiments on both synthetic datasets and real-world datasets, we compare our approach with a cheapest-insertion heuristic as the baseline. The experimental results demonstrate that our approach has significantly improved running-time while achieving comparable or sometimes significantly better solution quality, with the added benefit of having a provable worst-case performance guarantee.

Acknowledgments

This research was supported by data provided by Meituan.

References

- [1] Aaron Archer, MohammadHossein Bateni, MohammadTaghi Hajiaghayi, and Howard Karloff. Improved approximation algorithms for prize-collecting Steiner tree and TSP. *SIAM Journal on Computing*, 40(2):309–332, 2011. doi:10.1137/090771429.
- [2] Andreas Bärtschi, Jérémie Chalopin, Shantanu Das, Yann Disser, Daniel Graf, Jan Hackfeld, and Paolo Penna. Energy-efficient delivery by heterogeneous mobile agents. In *34th Symposium on Theoretical Aspects of Computer Science (STACS 2017)*, volume 66 of *Leibniz International Proceedings in Informatics (LIPIcs)*, pages 10:1–10:14. Schloss Dagstuhl – Leibniz-Zentrum für Informatik, 2017. doi:10.4230/LIPIcs.STACS.2017.10.
- [3] Andreas Bärtschi, Daniel Graf, and Matúš Mihalák. Collective fast delivery by energy-efficient agents. In *43rd International Symposium on Mathematical Foundations of Computer Science (MFCS 2018)*, volume 117 of *Leibniz International Proceedings in Informatics (LIPIcs)*, pages 56:1–56:16. Schloss Dagstuhl – Leibniz-Zentrum für Informatik, 2018. doi:10.4230/LIPIcs.MFCS.2018.56.
- [4] Iago A Carvalho, Thomas Erlebach, and Kleitos Papadopoulos. On the fast delivery problem with one or two packages. *Journal of Computer and System Sciences*, 115:246–263, 2021. doi:10.1016/J.JCSS.2020.09.002.
- [5] Jérémie Chalopin, Shantanu Das, Matúš Mihalák, Paolo Penna, and Peter Widmayer. Data delivery by energy-constrained mobile agents. In *9th International Symposium on Algorithms and Experiments for Sensor Systems, Wireless Networks and Distributed Robotics (ALGOSENSORS 2013)*, volume 8243 of *Lecture Notes in Computer Science*, pages 111–122. Springer, 2014. doi:10.1007/978-3-642-45346-5_9.
- [6] Jérémie Chalopin, Riko Jacob, Matúš Mihalák, and Peter Widmayer. Data delivery by energy-constrained mobile agents on a line. In *41st International Colloquium on Automata, Languages, and Programming (ICALP 2014)*,

Part II, volume 8573 of *Lecture Notes in Computer Science*, pages 423–434. Springer, 2014. doi:10.1007/978-3-662-43951-7_36.

- [7] Jérémie Chalopin, Shantanu Das, Yann Disser, Arnaud Labourel, and Matúš Mihalák. Collaborative delivery on a fixed path with homogeneous energy-constrained agents. *Theoretical Computer Science*, 868:87–96, 2021. doi:10.1016/j.tcs.2021.04.004.
- [8] Mark de Berg, Otfried Cheong, Marc J. van Kreveld, and Mark H. Overmars. *Computational geometry: Algorithms and applications, 3rd Edition*. Springer, 2008. doi:10.1007/978-3-540-77974-2.
- [9] Thomas Erlebach, Kelin Luo, and Frits C.R. Spieksma. Package delivery using drones with restricted movement areas. In *33rd International Symposium on Algorithms and Computation (ISAAC 2022)*, volume 248 of *Leibniz International Proceedings in Informatics (LIPIcs)*, pages 49:1–49:16. Schloss Dagstuhl – Leibniz-Zentrum für Informatik, 2022. doi:10.4230/LIPIcs.ISAAC.2022.49.
- [10] Greg N Frederickson, Matthew S Hecht, and Chul E Kim. Approximation algorithms for some routing problems. In *17th Annual Symposium on Foundations of Computer Science (SFCS 1976)*, pages 216–227. IEEE, 1976. doi:10.1109/SFCS.1976.6.
- [11] Michel X Goemans and David P Williamson. A general approximation technique for constrained forest problems. *SIAM Journal on Computing*, 24(2):296–317, 1995. doi:10.1137/S0097539793242618.
- [12] Meituan. Meituan INFORMS TSL research challenge. <https://github.com/meituan/Meituan-INFORMS-TSL-Research-Challenge>, 2026. GitHub repository, accessed 2026-02-09.
- [13] Sivakumar Rathinam, R Ravi, J Bae, and Kaarthik Sundar. Primal-dual 2-approximation algorithm for the monotonic multiple depot heterogeneous traveling salesman problem. In *17th Scandinavian Symposium and Workshops on Algorithm Theory (SWAT 2020)*, volume 162 of *LIPIcs*, pages 33:1–33:13. Schloss Dagstuhl - Leibniz-Zentrum für Informatik, 2020. doi:10.4230/LIPIcs.SWAT.2020.33.
- [14] Martin Savelsbergh and Tom Van Woensel. 50th anniversary invited article – City logistics: Challenges and opportunities. *Transportation Science*, 50(2):579–590, 2016. doi:10.1287/TRSC.2016.0675.

A Experimental Results on SY-GMM

In this appendix, we report additional experimental results on a synthetic dataset generated using a Gaussian Mixture Model, referred to as SY-GMM.

This synthetic benchmark is used to evaluate the performance of the proposed methods under controlled and varied conditions, complementing the experiments presented in the main part of the paper.

Figures 15, 16, and 17 summarize the experimental results on the SY-GMM dataset. Overall, the results exhibit trends consistent with those observed on the synthetic uniform dataset. These findings indicate that the proposed methods are robust to variations in spatial request distribution and scale favorably with increasing problem size, reinforcing the conclusions of this work.

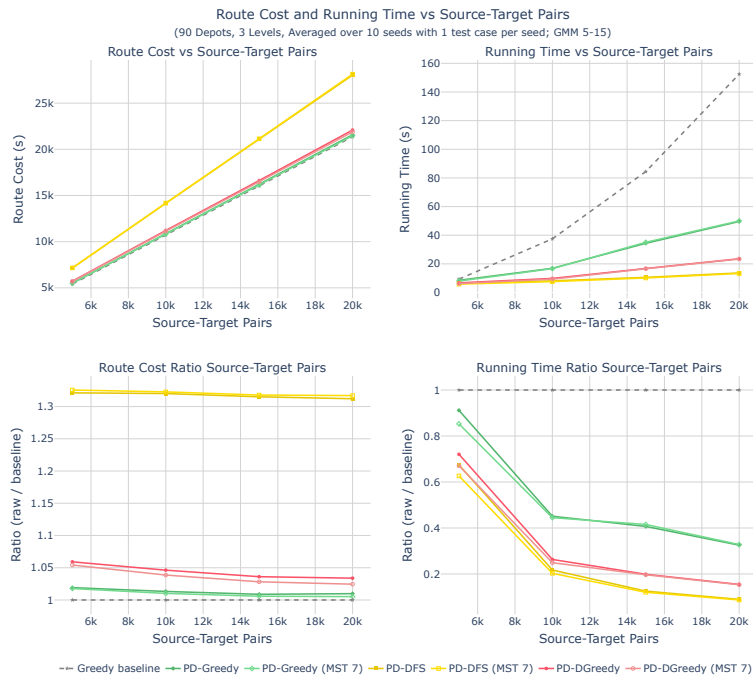


Figure 15: Results on the SY-GMM with varying n .

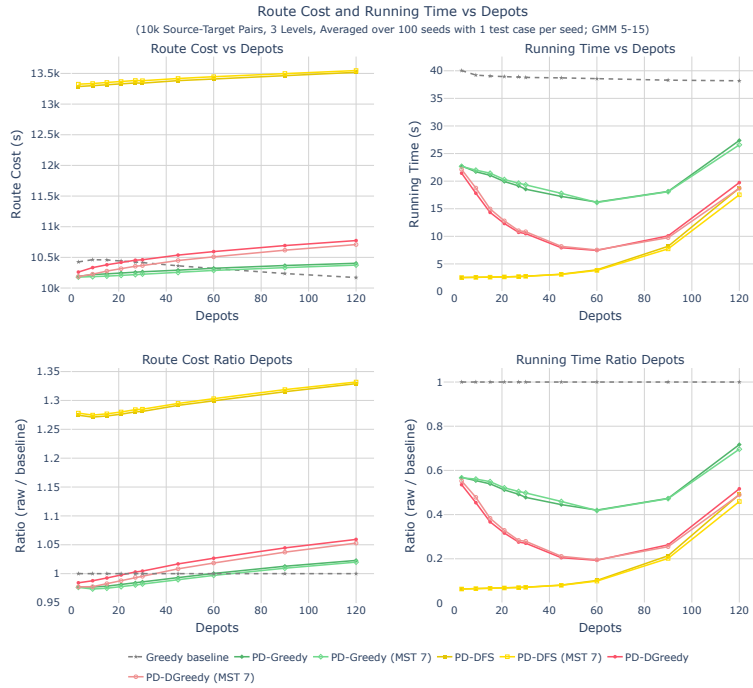


Figure 16: Results on the SY-GMM with varying k .

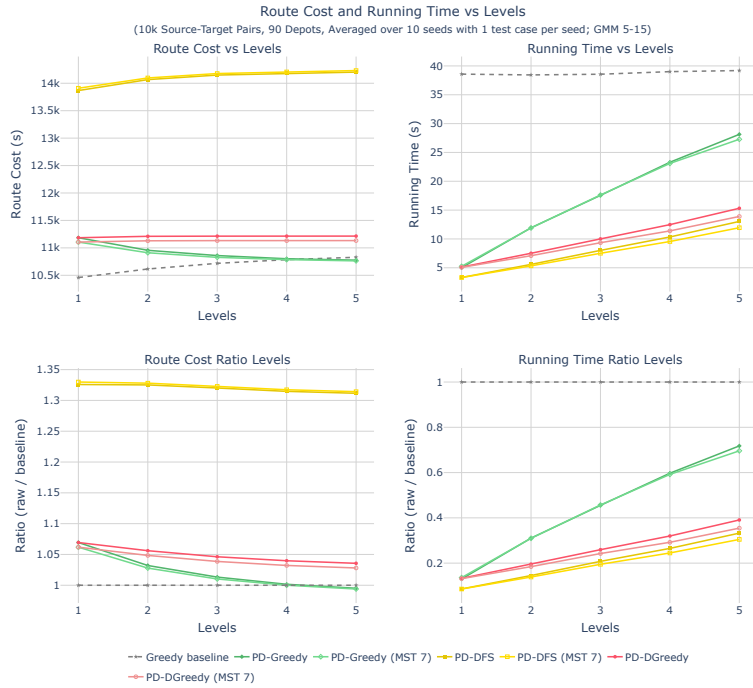


Figure 17: Results on the SY-GMM with varying h .